



McGill University, MacDonald Campus
Department of Bioresource Engineering

BREE 495 – Engineering Design 3

AN INNOVATIVE WASTEWATER TREATMENT SYSTEM DESIGN FOR A FOOD FACILITY

Group 4 – AiroLeaders

Jun Dong (260442997)

Zhi Li (260331791)

Erbolat Riskulov (260483038)

Dillon Stanger (260411556)

Presented to:

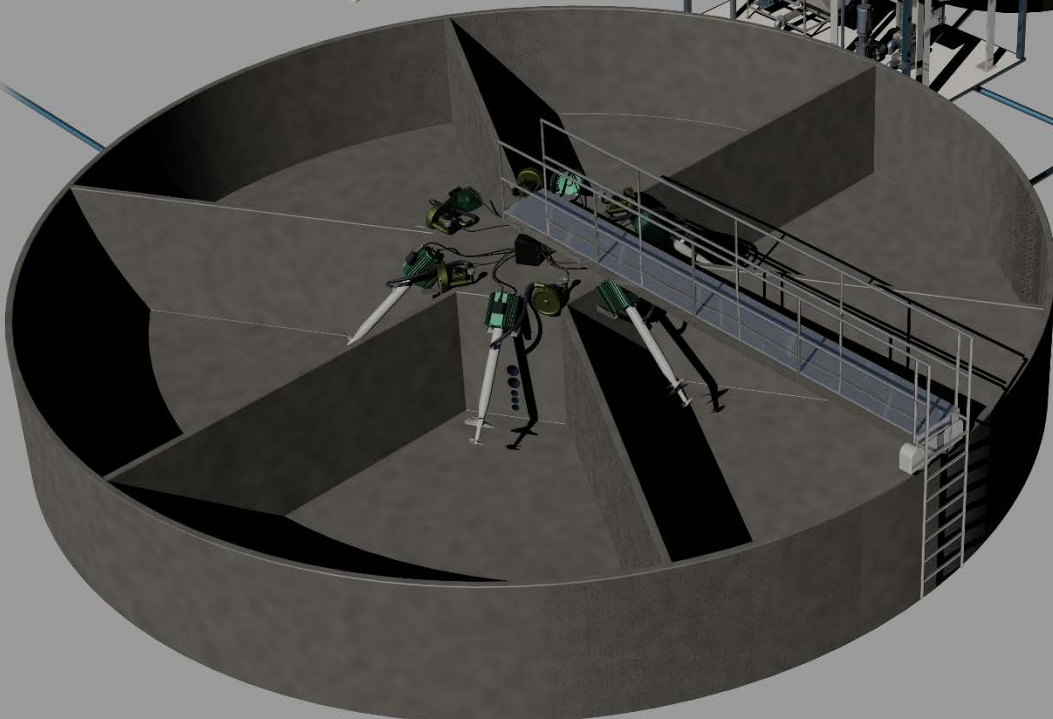
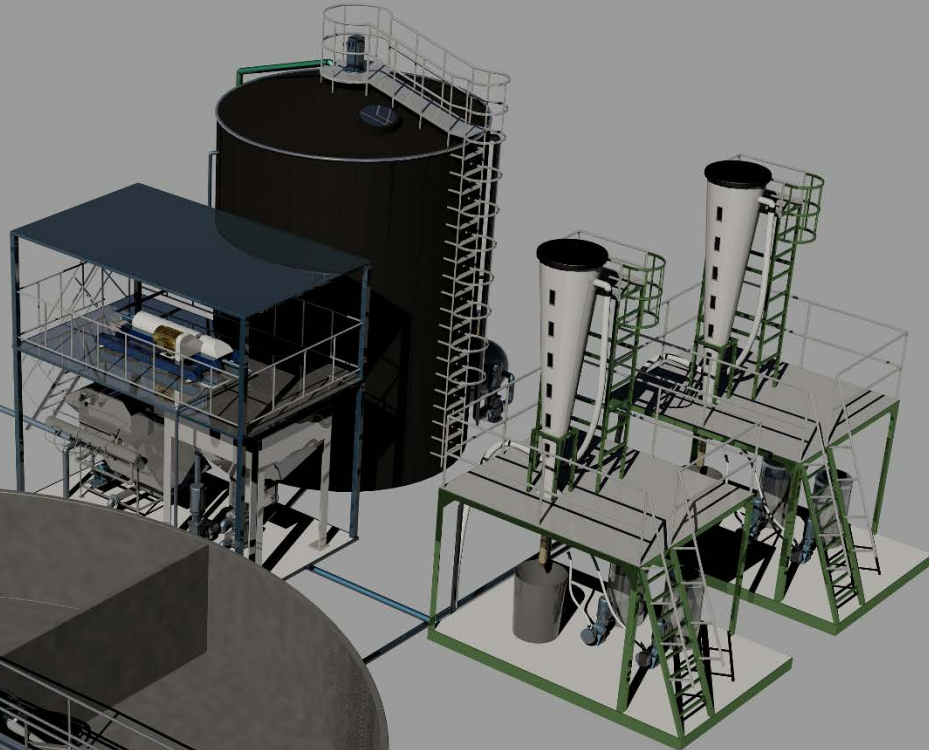
Prof. Grant Clark (McGill)

Mr. Ignacio Riera (Mabarex)

Mr. Jean-Philippe Raboud (Mabarex)

18 April 2014

mabarex



Executive Summary

An innovative wastewater treatment system was designed for an un-disclosed slaughterhouse in Montreal for the reduction of organics, nutrients, lipids and suspended solids while producing renewable energy. Furthermore, this design profits 200 000 \$ per year from valorising recovered nutrients rather than eliminating them at cost as normal wastewater treatment plants do. The system components include a dissolved air floatation unit, a dual-cycle sequencing batch reactor, an anaerobic sludge digester, and two struvite precipitators. The design is reviewed by two professional wastewater engineers from our client Mabarex Inc.

Table of Contents

Executive Summary.....	1	DAF Unit	22
Abbreviations.....	2	Dual-Cycle SBR.....	23
Introduction.....	3	SBR Mixing and Aeration.....	27
Problem Statement	3	SBR pH Control	27
Objectives	3	Anaerobic Sludge Digester	28
Analysis and Specifications.....	3	Centrifuge.....	28
Treatment System	3	Struvite Precipitator	29
DAF Unit.....	4	Testing and Optimisation	30
Dual-Cycle SBR.....	6	Safety and Economics.....	31
SBR Mixing and Aeration	12	Environmental Safety	31
SBR pH Control.....	14	Occupational Health and Safety.....	32
Anaerobic Sludge Digester	14	Economics.....	32
Centrifuge	17	Conclusion.....	33
Struvite Precipitator	18	Design Paper Competition	34
Pumping.....	20	Acknowledgements.....	34
Simulation and Optimisation.....	21	References.....	35
Influent	22		

Abbreviations

Actual oxygen transfer rate	AOTR
Bio-soluble chemical oxygen demand	bsCOD
Chemical oxygen demand	COD
Day(s)	d
Dissolved air floatation	DAF
Dissolved oxygen	DO
Fat, oil and grease	FOG
Flow rate	Q
Hour(s)	h
Mean hydraulic retention time	HRT
Nitrogen	N
Nitrogen in form of ammonium	N-NH ₄
Nitrogen in form of nitrate	N-NO ₃
Non-soluble chemical oxygen demand	nsCOD
Phosphorus	P
Phosphorus in forms of phosphates	P-PO ₄
Safety factor	SF
Sequencing batch reactor	SBR
Soluble chemical oxygen demand	sCOD
Standard oxygen transfer efficiency	SOTE
Standard oxygen transfer rate	SOTR
Sulfur	S
Sulfur in form of hydrogen sulfide	S-H ₂ S
Sulfur in form of sulfate	S-SO ₄
Temperature	T
Total Kjeldhal nitrogen	TKN
Visual basic for applications	VBA
Volatile suspended solids	VSS

Introduction

Problem Statement

Due to the new stringent bylaw from the Montreal Metropolitan Community concerning industrial wastewater discharging into the municipal sewage, a food processing facility (confidential) in Montreal is required to implement a wastewater treatment system for its three effluents. These three wastewater streams are combined into one inside an equalisation tank providing a stable wastewater flow of 113 m³/d. The wastewater conditions and the bylaw limits (CMM, 2008) are listed in Table 1:

Table 1. Wastewater conditions and bylaw limits

Criteria	Wastewater	Bylaw
Q (m ³ d ⁻¹)	113	N/A
COD (g m ⁻³)	7804	800
TKN (g m ⁻³)	2063	70
N-NH ₄ (g m ⁻³)	1530	45
P-PO ₄ (g m ⁻³)	66	20
S-H ₂ S (g m ⁻³)	13	5
FOG (g m ⁻³)	661	250
VSS (g m ⁻³)	417	500
T (°C)	68	65
pH	6.7	6.0 – 11.5

The COD is an indication of organics content in water. The COD characteristics are covered in Table 2.

Table 2. COD characteristics

sCOD/COD	37%
bsCOD/COD	32%
nsCOD/COD	63%

The NTK is the total nitrogen in forms of ammonium (NH₄⁺) and proteins in the wastewater. The phosphorus exists as orthophosphate (PO₄³⁻) and polyphosphates (PO₄⁻)_n. The sulfur is regarded as sulfide species that are biologically and chemically convertible into hydrogen sulfide. The FOG represents the total lipids in water and, finally, the primary VSS are mainly fine meat particles, which are

made of COD, TKN, P, S and FOG, suspended in the wastewater.

The food factory sought a solution to the problem from our client Mabarex Inc., an engineering consulting firm located in Montreal, specialized in wastewater treatment. Graciously, our mentors, Ignacio Riera, Eng., M. Eng. and Jean-Philippe Raboud, Eng., Ph.D., from our client Mabarex provided us with this problem for a design study.

Objectives

The primary objective of this project is to design a wastewater treatment system able reduce contaminants below their bylaw limits. As an additional challenge to the problem, the slaughterhouse is interested to recover and valorise the wastes and nutrients (N and P) from the wastewater treatment.

Analysis and Specifications

This analysis section will firstly present the system process schematic with description in broad terms. Next, mathematical models and equations will be explained for specifying and designing every system component. The system components were preliminarily specified in writing or in drawings in millimetre unit. Details concerning design, simulation, and optimisation will be presented in the section of Simulation and Optimisation.

Treatment System

The design of the treatment process or system (Figure 1) was limited to: (1) to ensure that all the contaminants are treated below their bylaw limits, (2) to recover as much as possible the nutrients (N and P) from the water and valorise them as fertilisers in order to improve the operational economy, and (3) to consider for some of the environmental and safety issues.

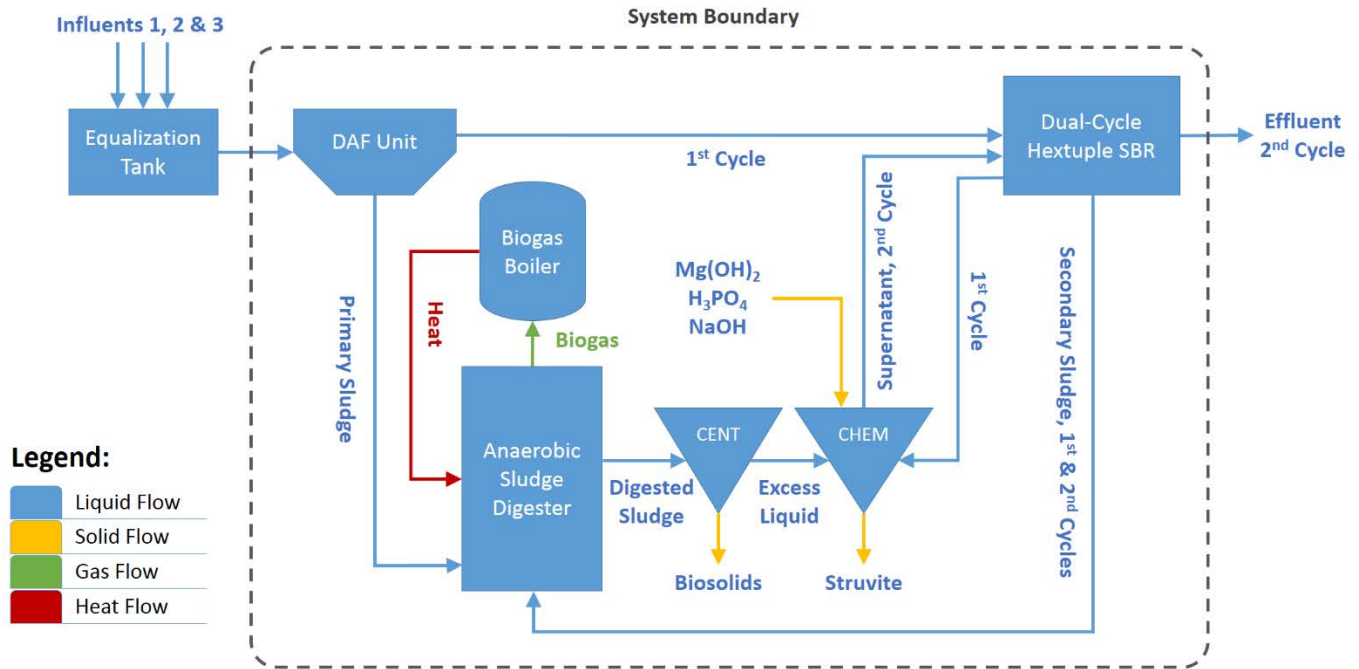


Figure 1. The components are shown in the blue colored blocks and the arrow lines represent the water flow and the interactions between the components

As seen from Figure 1, the combined wastewater streams are pumped from the flow equalization tank at the rate of $113 \text{ m}^3 \text{ d}^{-1}$. The combined flow travels through the DAF unit to begin the physical removal of non-soluble contaminants. These contaminants include most of the FOG and the VSS along with some other constituent contaminants (such as COD, TKN, P, and S). The wastewater then flows from the DAF to the dual-cycle SBR to perform an anoxic cycle and an aerobic cycle activated sludge (biological or microbial) treatment processes. In simple terms, the anoxic cycle is designed to isolate the soluble ammonium and phosphate in water. The nutrients from the anoxic effluent is then pumped to the chemical precipitator (CHEM from Figure 1) for recovery in form of struvite, which is a natural mineral fertilizer that contains ammonium, phosphate and magnesium (details about struvite on page 31). At the same time, the sludge from the DAF and the SBR are sent to the anaerobic sludge digester for three purposes. Firstly, it biologically converts the carbon content from the sludge into

around 65% of collectable methane as a renewable energy source and 30% carbon dioxide (Tchobanoglous et al., 2003). This method emits less methane, a strong greenhouse gas, than the landfill disposal of sludge. Secondly, the digestion produces biosolids from the digested sludge remains as a fertilizer. The biosolids suspended in the liquid is then physically separated by a centrifuge (CENT from Figure 1) following the digester. Thirdly, the digestion of sludge releases more N and P into the liquid so that extra nutrients will be recovered in the struvite precipitator. After the nutrient recovery, the supernatant fluid that contains some residual contaminants (bsCOD, TKN, P- PO_4 , H_2S , FOG and VSS) is returned to the SBR for the second aerobic cycle treatment before the final effluent is discharged.

DAF Unit

This project specified to select a pre-fabricated DAF unit from a supplier named Piedmont Technical Services or P-TEC. P-TEC designed their DAF unit with standard volumes based on a standard HRT of

treatment. Therefore, the DAF unit was selected by the flow rate as defined in Eq. 1

Flow rate is related to volume and HRT as:

$$Q = \frac{V}{HRT} \quad (1)$$

where

Q = wastewater flow rate ($m^3 d^{-1}$)

V = volume (m^3)

HRT = mean hydraulic retention time, (d)

Based on the flow rate, the P-TEC MicroDAF 36-42 model (P-TEC, 2014), which is shown in Figure 2 and Figure 3, was chosen to be the DAF unit. Moreover, the air pressure for the DAF process is specified with the air-to-solid (A-S ratio) equation defined in Eq. 2 (Tchobanoglous et al., 2003). For the optimal non-soluble contaminant removals, a DAF unit from

slaughterhouses was recommended to specify an A-S ratio of $0.03 L g^{-1}$ (De Nardi, 2008), resulting an operational air pressure of 4 atm. This pressure will ensure the generation of adequately sized micro-bubbles that attach to the VSS particles in the wastewater and lift them along with the FOG to the top of the DAF unit where they will be skimmed off.

The air-to-solid ratio is defined as:

$$\frac{A}{S} = \frac{1.3s_a(fP - 1)}{S} \quad (2)$$

where

$\frac{A}{S}$ = Air to solid ratio ($L g^{-1}$)

s_a = air solubility in water ($mL L^{-1}$)

P = pressure (atm)

f = dissolved air fraction at P (typically 0.5)

S = influent VSS concentration ($mg L^{-1}$)

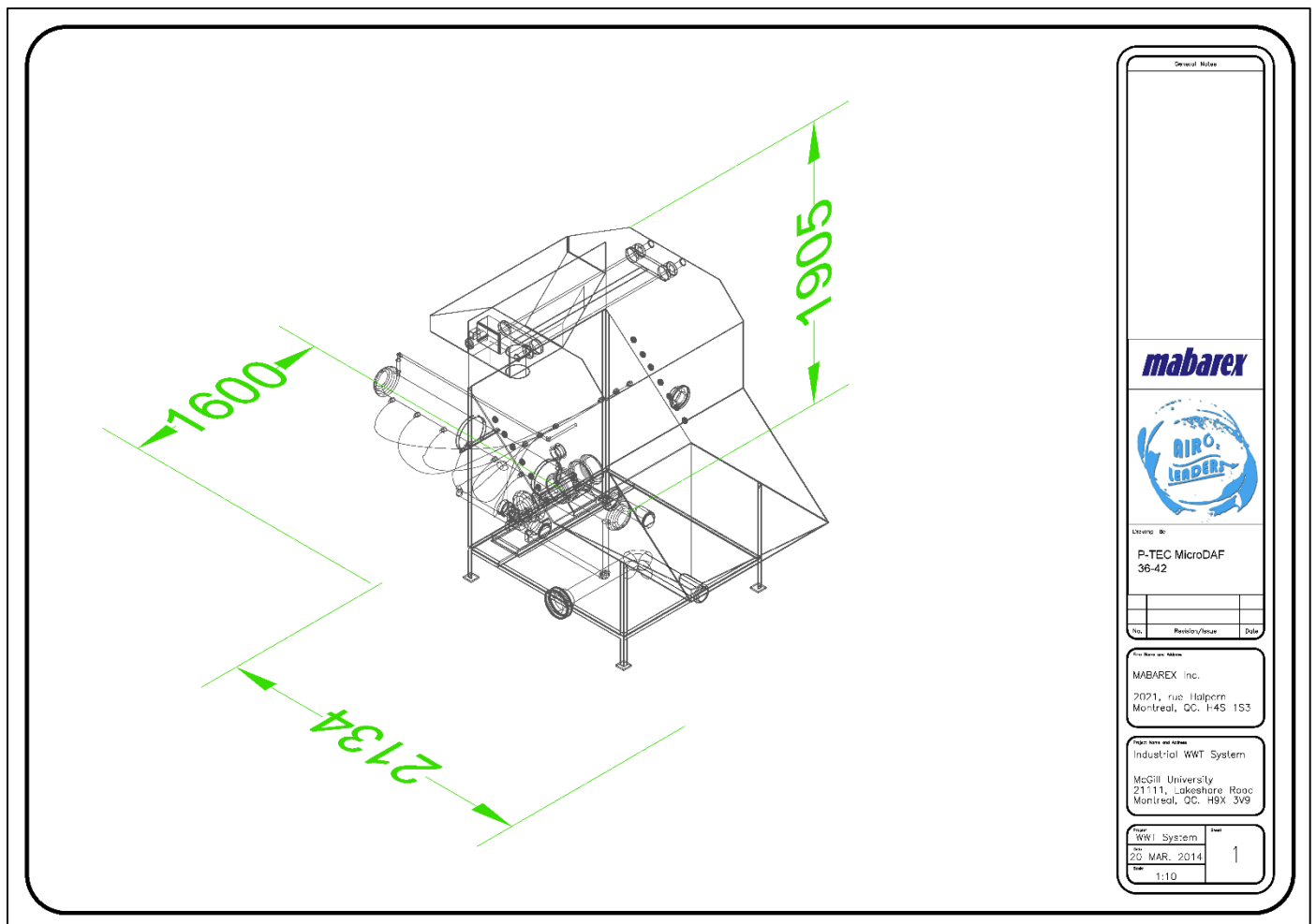


Figure 2. Drawing of the DAF unit with important axial dimensions of extremity (by Erbolat Riskulov)



Figure 3. Illustration of the supplied P-TEC MicroDAF 36-42 (by Erbolat Riskulov and Jun Dong)

Dual-Cycle SBR

The dual-cycle SBR, as mentioned in the Treatment System section on page 4, was specifically designed to run two cycles. The reason for the dual-cycle design was to be able to extract the rich amount of ammonium dissolved in the water before it is eliminated. The ammonium cannot be precipitated before the SBR along with other contaminants such as the bsCOD, VSS and FOG because these contaminants can introduce impurities (suspended solids) into the precipitated struvite and damage the equipment. Consequently, an anoxic cycle (Figure 4)

was designed as the treatment cycle of the SBR to remove those unwanted contaminants.

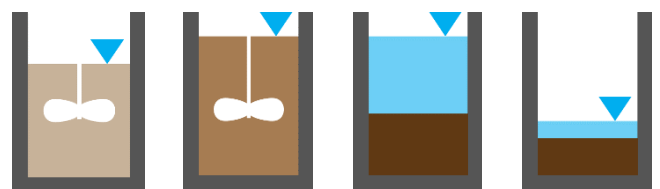


Figure 4. An illustration of the anoxic cycle processes, which are the anoxic fill, the anoxic reaction, the settling and the discharge (decant), presented in the order from left to right (by Jun Dong).

Upon the completion of the anoxic cycle, most of the effluent with high NH_4^+ and PO_4^{3-} contents is slowly pumped to the struvite precipitator where it is combined with the effluent coming from the anaerobic sludge digester that also contains some concentrated NH_4^+ , PO_4^{3-} and some residual bsCOD that the precipitator can handle (Bowers, 2007). However, due to the streams combination, the bsCOD from the anaerobic effluent is diluted by the anoxic effluent so that the precipitation condition is improved. After the NH_4^+ and PO_4^{3-} are recovered from the struvite precipitator, the supernatant with the diluted bsCOD and residual ammonium and phosphate are returned to the SBR. Thus, the returned supernatant is contaminated with the remaining untreated TKN, P- PO_4 and S- H_2S by the sludge left from the anoxic cycle (the decant stage from Figure 4). Consequently, these contaminants will be practically treated with an aerobic activated sludge process that is shown in Figure 5 (Sharma, 2010; Tchobanoglous et al., 2003).

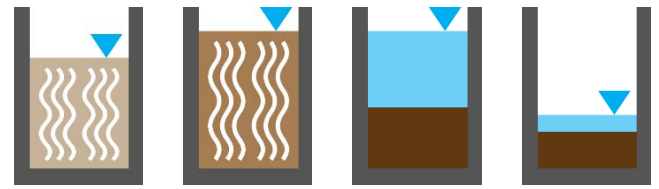


Figure 5. An illustration of the aerobic cycle processes including the aerobic fill, the aerobic reaction, the settling and the discharge presented in the order from left to right (by Jun Dong).

Figure 6 below is an illustration of the interactions between the SBR processes and the contaminants for specifications. Inside a single SBR compartment, the first anoxic denitrification process starts since the anoxic fill stage where the influent is pumped in and stirred with the denitrifiers specified at $3000 \text{ g VSS m}^{-3}$ within the sludge under an average anoxic condition of 0.25 g DO m^{-3} (Tchobanoglous et al., 2003). When the reactor is filled, the inflow will be driven to another compartment, whereas the filled compartment is now into the reaction stage where the denitrification is continued.

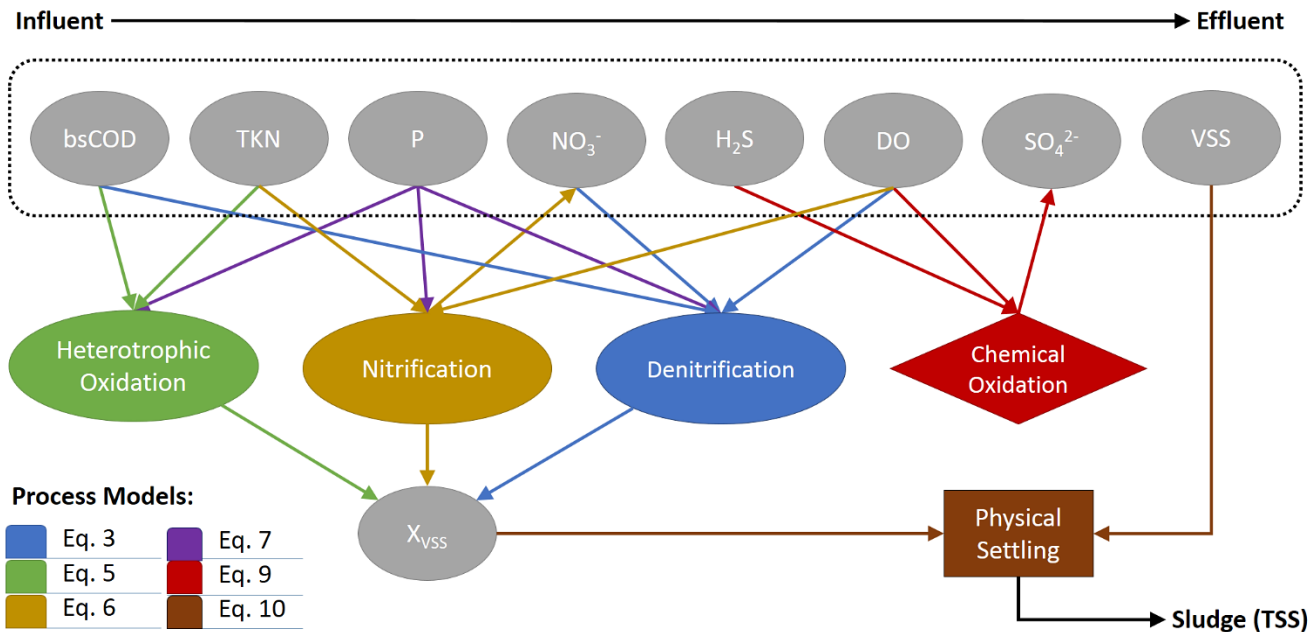


Figure 6. The biological, chemical and physical processes within the SBR interact with the contaminants. Each of the process is color-coded with a corresponding mathematical model. The microorganisms can practically survive in the SBR switching between the anoxic and the aerobic conditions (by Jun Dong).

The denitrifiers thrive in the presence of nitrate (electron acceptor) and bsCOD organics (electron donor and carbon source) while being inhibited by the increasing amount of DO. As such, the biokinetics of denitrifiers at 20°C are governed by Eq. 3 (Tchobanoglous et al., 2003). This mathematical model simulated the minimum denitrification process timing, the sludge production, and the bsCOD, N-NO₃, and P-PO₄ concentrations from the anoxic effluent.

The Monod equation for denitrificant biokinetics:

$$\frac{\partial X_{DN}}{\partial t} = X_{DN} \left[\left(\frac{\mu_{m,DN} NO_3}{K_{DN} + NO_3} \right) \left(\frac{S}{K_{DN,S} + S} \right) \left(\frac{K_o'}{K_o' + DO} \right) - k_{d,DN} \right] \quad (3a)$$

$$\frac{\partial NO_3}{\partial t} = -X_{DN}(SDNR) \quad (3b)$$

$$\frac{\partial S}{\partial t} = - \left(\frac{1}{Y_{DN}} \right) \frac{\partial X_{DN}}{\partial t} \quad (3c)$$

where

X_{DN} = denitrifiers concentration (g VSS m⁻³)

t = time (d)

$\mu_{m,DN}$ = maximum denitrifiers specific growth rate (3.2 d⁻¹)

NO_3 = nitrate nitrogen concentration (g N-NO₃ m⁻³)

K_{DN} = denitrifiers nitrate half-rate constant (0.1 g NO₃⁻ m⁻³)

S = substrate concentration (g bsCOD m⁻³)

$K_{DN,S}$ = denitrifiers substrate half-rate constant (9 g S m⁻³)

K_o' = DO inhibition concentration (0.11 g DO m⁻³)

DO = denitrification dissolved oxygen (0.25 g DO m⁻³)

$k_{d,DN}$ = denitrifiers death rate (0.15 g VSS g⁻¹ VSS d⁻¹)

$SDNR$ = specific denitrification rate (g N-NO₃ g⁻¹ VSS d⁻¹)

Y_{DN} = denitrifiers yield on bsCOD (0.4 g VSS g⁻¹ bsCOD)

From Eq. 3, the specific denitrification rate ($SDNR$) varies with the food-to-microorganism ratio (F/M) that is defined by Eq. 4 (Tchobanoglous et al., 2003).

The food-to-microorganism ratio is defined as:

$$\frac{F}{M} = \frac{QS_o}{VX_{VSS}} \quad (4)$$

where

F/M = food-to-microorganism ratio (g bsCOD g⁻¹ VSS d⁻¹)

Q = wastewater flow rate (m³ d⁻¹)

S_o = initial substrate concentration (g bsCOD m⁻³)

V = reactor volume (m³)

X_{VSS} = microbial concentration (g VSS m⁻³)

For the aerobic process, the returned supernatant is mixed aerobically with the aerobes from the sludge and the contaminant treatments begin. Two groups of aerobes are performing the second aerobic treatment. Referred to Figure 6, the first group is the heterotrophs and it is responsible for the biological oxidation of bsCOD carbons and the bio-assimilation of TKN and P-PO₄. The growth rate for heterotrophs relies on the substrate or bsCOD level, yet the growth is insensible to the DO levels afforded by the standard aerations. Hence, the heterotrophic biokinetics at 20°C are described by Eq. 5 (Riera, 2013; Tchobanoglous et al., 2003). This model simulated the aeration timing, the removals of bsCOD, TKN and P, and the sludge production.

The Monod equation for heterotrophic biokinetics:

$$\frac{\partial X_S}{\partial t} = X_S \left(\frac{\mu_{m,S} S}{K_S + S} - k_{d,S} \right) \quad (5a)$$

$$\frac{\partial S}{\partial t} = - \left(\frac{1}{Y_S} \right) \frac{\partial X_S}{\partial t} \quad (5b)$$

$$\frac{dN}{dt} = -n \frac{dX_S}{dt} \quad (5c)$$

where

X_S = heterotrophs concentration (g VSS m⁻³)

t = time (d)

$\mu_{m,S}$ = maximum heterotrophs specific growth rate (6.0 d⁻¹)

S = substrate concentration (g bsCOD m⁻³)

K_S = heterotrophs half-rate constant (20 g bsCOD m⁻³)

$k_{d,S}$ = heterotrophs death rate (0.12 g VSS g⁻¹ VSS d⁻¹)

Y_S = heterotrophs yield on bsCOD (0.4 g VSS g⁻¹ bsCOD)

N = TKN concentration (g N m⁻³)

n = nitrogen assimilation ratio (0.12 g TKN g⁻¹ VSS)

Another group of the aerobes, from Figure 6, is the nitrifiers. The nitrifiers are mostly chemoautotrophs, meaning that they use ammonium as their energy source while fixing carbon dioxide for their carbon and oxygen sources. The carbon dioxide is brought by the aeration that is correlated to the DO level. Besides, recall from Figure 6 that denitrification requires nitrate. That nitrate is produced here in the aerobic cycle after the ammonium is biologically

oxidized by the nitrifiers. As such, the biokinetics of the nitrifiers at 20°C are modeled as Eq. 6 (Tchobanoglous et al., 2003). The nitrifying biokinetics simulated the aeration timing, the TKN removal and the sludge production.

The Monod equation for nitrifying biokinetics:

$$\frac{\partial X_N}{\partial t} = X_N \left[\left(\frac{\mu_{m,N} N}{K_N + N} \right) \left(\frac{DO}{K_O + DO} \right) - k_{dN} \right] \quad (6a)$$

$$\frac{\partial N}{\partial t} = - \left(\frac{1}{Y_N} \right) \frac{\partial X_N}{\partial t} \quad (6b)$$

where

X_N = nitrifiers concentration (g VSS m⁻³)

t = time (d)

$\mu_{m,N}$ = maximum nitrifiers specific growth rate (0.75 d⁻¹)

N = TKN concentration (g N m⁻³)

K_N = nitrifiers TKN half-rate constant (0.74 g N m⁻³)

DO = dissolved oxygen concentration (3 g DO m⁻³)

K_O = nitrifiers DO half-saturation constant (0.5 g DO m⁻³)

k_{dN} = nitrifiers death rate (0.08 g VSS g⁻¹ VSS d⁻¹)

Y_N = nitrifiers yield on TKN (0.12 g VSS g⁻¹ N)

Furthermore, Figure 6 shows that phosphorus is assimilated by all group of microbes into their cell tissue. The assimilation of P by the microbes can be estimated by Eq. 7 (Riera, 2013).

The bio-assimilation of phosphorus by microbes:

$$\frac{dP}{dt} = -p \frac{dX}{dt} \quad (7)$$

where

P = phosphorus concentration (0.02 g P m⁻³)

t = time (d)

p = phosphorus assimilation ratio (g P g⁻¹ VSS)

X = microbial concentration (g VSS m⁻³)

Moreover, some of the biokinetics parameters depend significantly on the temperature. Those parameters can be corrected to the actual temperature of the water during the process by Eq. 8 (Tchobanoglous et al., 2003).

Temperature correction of different reaction rates:

$$k_T = k_{20} \theta^{T-20^\circ\text{C}} \quad (8)$$

where

k_T = temperature corrected reaction rate (g g⁻¹ d⁻¹)

k_{20} = standard reaction rate at 20°C (g g⁻¹ d⁻¹)

θ = temperature coefficient (unitless)

T = actual temperature (°C)

In addition, during the aerobic process, the S-H₂S is chemically oxidized into S-SO₄. The hydrogen sulfide oxidation kinetics modeled for a SBR at 20°C is presented in Eq. 9 (Sharma, 2010) for simulating the aeration timing and the final S-H₂S level.

The Monod hydrogen sulfide oxidation kinetics:

$$\frac{d[S_{H_2S}]}{dt} = -k[S_{H_2S}]^\alpha \left(\frac{DO}{K_O + DO} \right) \quad (9)$$

where

$[S_{H_2S}]$ = sulfur concentration as H₂S (g S m⁻³)

t = time (d)

k = specific oxidation rate (107 d⁻¹)

α = pseudo reaction order (0.56 unitless)

DO = dissolved oxygen concentration (g DO m⁻³)

K_O = DO half-rate concentration (13 g DO m⁻³)

After the completion of the anoxic or aerobic process, the mixer or aerator is then turned off to allow the sludge settling. The adopted mathematical model describing the physical sludge settling (Tchobanoglous et al., 2003) is presented in Eq. 10 for simulating the settling timing and the final suspended solids concentrations.

The adopted physical sludge-settling model:

$$\frac{dX_{VSS}}{dt} = - \frac{6.5X_{VSS}}{h_s} \exp[-(0.165 + 0.00159 SVI)X_{VSS}] \quad (10)$$

where

X_{VSS} = suspended solids concentration (kg VSS m⁻³)

t = time (h)

h_s = mean settling height (m)

SVI = sludge volume index (120 mL g⁻¹)

Once the sludge is settled, the effluent and the sludge are discharged simultaneously but separately. For each of the SBR treatment cycle, all the process timings must follow the rules stated in Eq. 11 to

achieve an overall continuous treatment within the entire system. However, as the denitrification process time might not be equal to the aerobic process time, one of the SBR cycle will have longer cycle time, so that the other cycle will have an extra idling time where the SBR compartment is completely at rest and where equipment maintenance can be scheduled and performed.

SBR process timing rules for continuous treatment:

$$t_I + t_F = t_R + t_S = t_D \quad (11a)$$

$$t_{AO} = t_F + t_R \quad (11b)$$

where

t_I = idling time (h)

t_F = fill time (h)

t_R = reaction time (h)

t_S = settling time (h)

t_D = discharge time (h)

t_{AO} = anoxic or aerobic process time (h)

To comply with the timing rules for a continuous process, six SBR compartments are required. Three of them work on the anoxic cycle with each at different sequences (idling and fill, reaction and settling, or decant) while the other three are working similarly but on the aerobic cycle. The compartment and the SBR were sized (Figure 7 and Figure 8) with the obtained process timings (Figure 9), the water flow rate, the sludge concentration, and the SVI.

Lastly, the flow rate of the sludge was adjusted with the sludge production rate and the allowable discharging time (t_D), so that content remains in equilibrium. By simulation, a $9.3 \text{ m}^3 \text{ d}^{-1}$ of sludge discharge flow was specified.

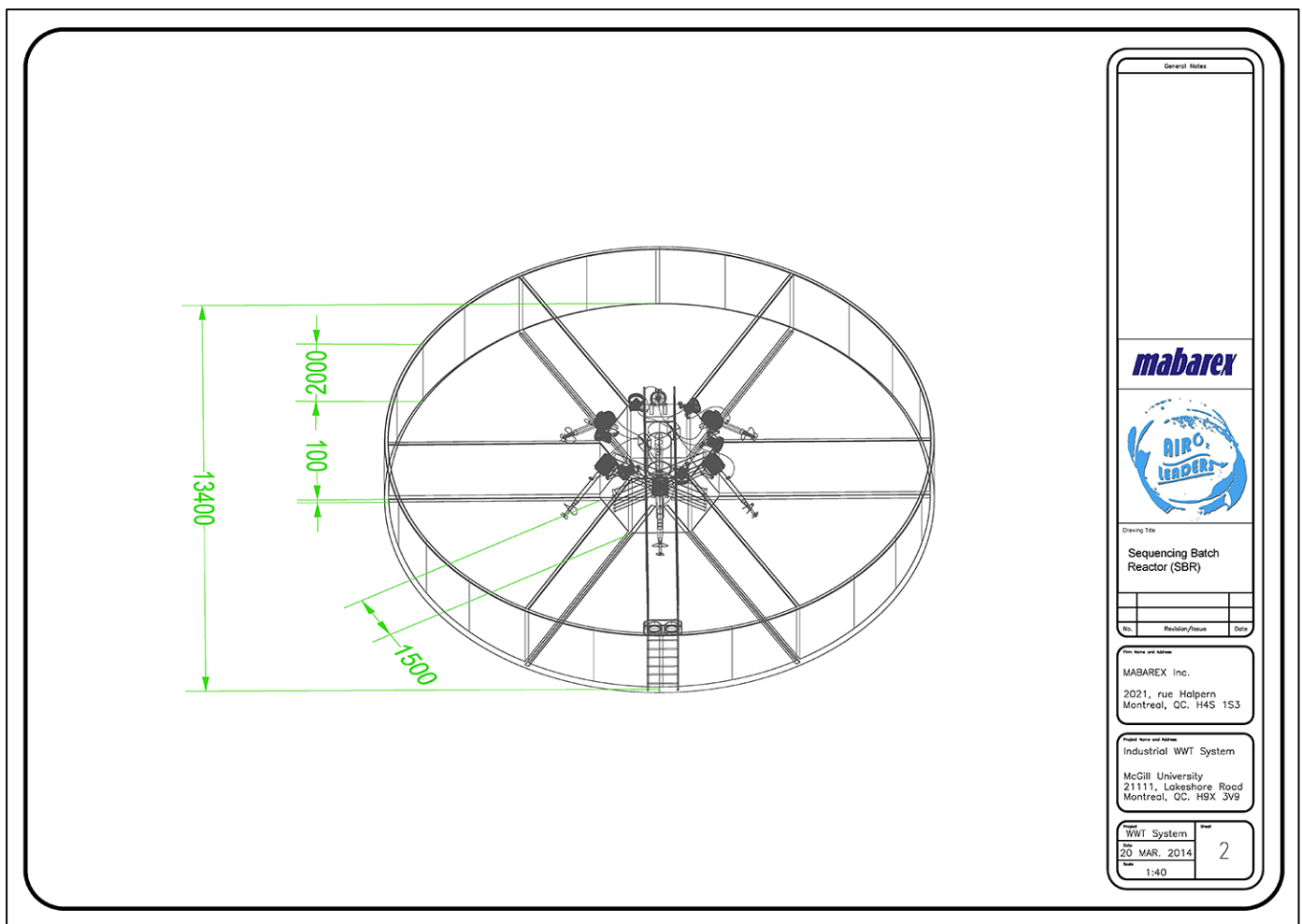


Figure 7. Drawing of the designed SBR with important construction dimensions (by Jun Dong)

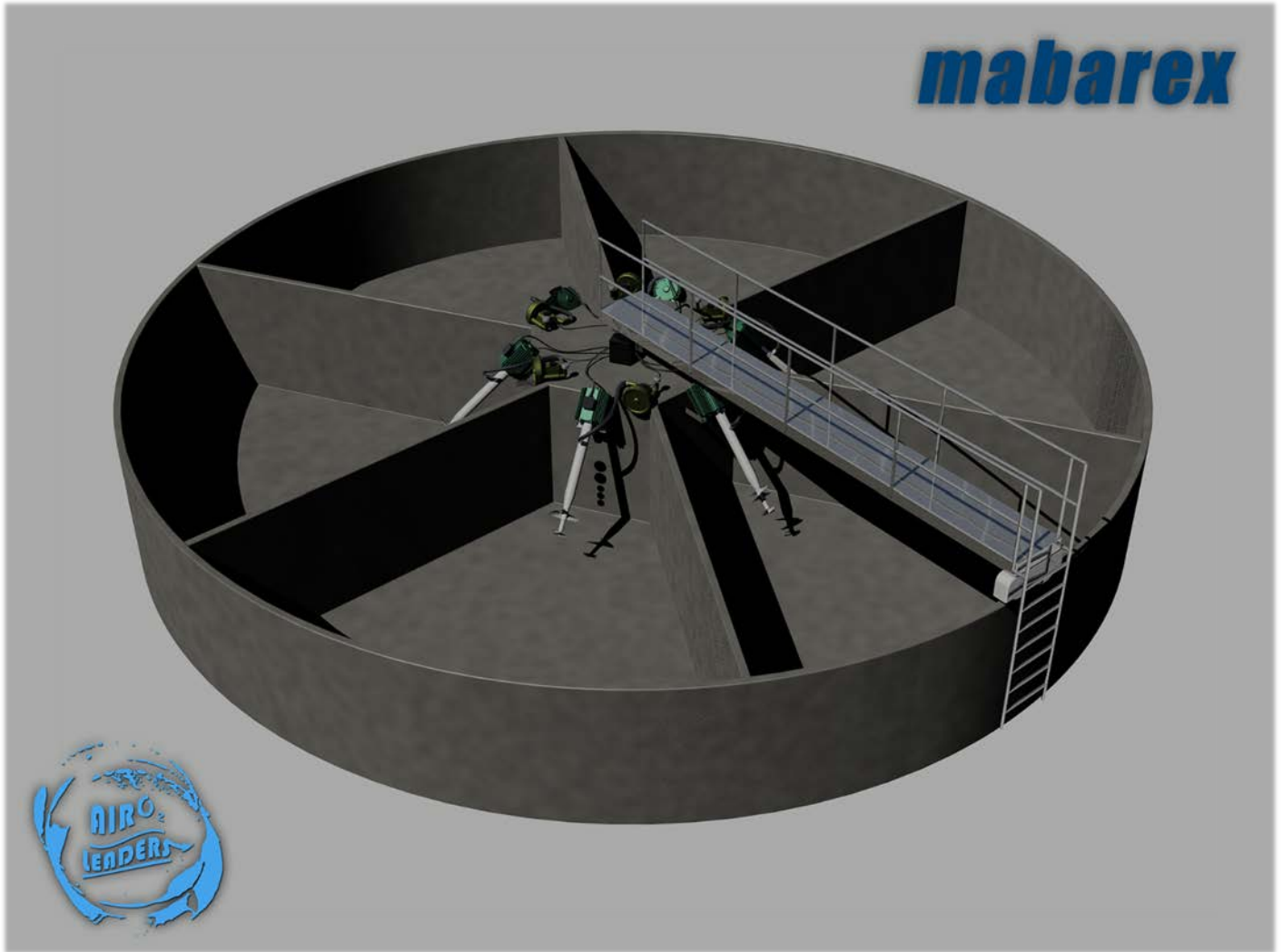


Figure 8. Mabarex Inc. provides the construction of the dual-cycle Hextuple compartment SBR (by Jun Dong)

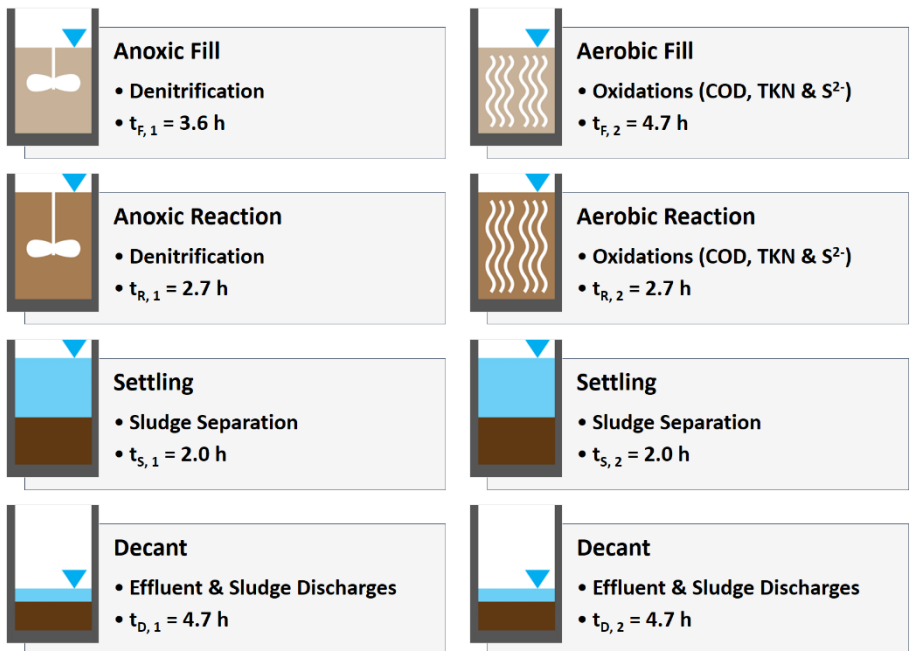


Figure 9. The anoxic and the aerobic process timings specified for the SBR. The denitrification time ($t_{F,1} + t_{R,1}$) is 6.3 h and the aerobic time ($t_{F,2} + t_{R,2}$) is 7.4 h. Furthermore, the difference between the two fill times is the idling time ($t_{F,2} - t_{F,1} = t_I = 1.1$ h) occurring before the anoxic cycle. Moreover, as each cycle takes 14.1 h, the period for the SBR to perform both cycles is 28.2 h.

SBR Mixing and Aeration

The Triton™ combined mixer and aerator from AIRE-O₂ Aeration Industries was chosen for the SBR as it provides both mixing and fine-bubble aeration functionalities for the anoxic and the aerobic cycles. Compared to typical dispersed air diffusers and surface aerators, the Triton™ is relatively easier to install and maintain; also, it does not splash microbes and odour into air, reducing occupational risks. By practical standards, the Triton™ can be wall mounted at a downward angle of 45°.

The selection of the Triton™ was by specifying the mixing and aeration powers. The mixing power is specified by Eq. 12 (Tchobanoglous et al., 2003).

The mixing power by velocity gradient:

$$P = G^2 \mu V \quad (12)$$

where

P = mixing power (W)

G = velocity gradient (typically 200 s⁻¹)

μ = dynamic viscosity (N s m⁻²)

V = reactor volume (m³)

To specify the aeration power, the AOTR (Eq. 13) is firstly calculated. It is then corrected to the SOTR by many specified factors as stated in Eq. 14 (MDDEFP, 2001; Stenstrom et al., 2010; Tchobanoglous et al., 2003). The SOTR is then converted by the SOTE, which is 0.12 kg air kg⁻¹ O₂, into the air mass flow (w) so that the standard blower power necessary for the aeration can be determined by Eq. 15 (Riera, 2013; Tchobanoglous et al., 2003).

The adopted AOTR equation:

$$AOTR = Q(\Delta S) - 1.42(P_{X,VSS}) + 4.33Q(\Delta NO_3) \quad (13)$$

where

$AOTR$ = actual oxygen transfer rate (g O₂ d⁻¹)

Q = wastewater flow rate (m³ d⁻¹)

ΔS = substrate consumption (g bsCOD m⁻³)

$P_{X,VSS}$ = sludge production rate (g VSS d⁻¹)

ΔNO_3 = nitrate yield due to nitrification (g N-NO₃ m⁻³)

The adopted SOTR equation:

$$\frac{AOTR}{SOTR} = \alpha \theta^{T-20^\circ C} \left(\frac{\beta C_{SW} - C_L}{C_{SS}} \right) \quad (14a)$$

$$C_{SW} = C_{ST} \left[\frac{P_b + 9.78(DWD)f}{101.3 \text{ kPa}} \right] \quad (14b)$$

$$C_{SS} = C_{S20} \left[\frac{101.3 \text{ kPa} + 9.78(DWD)f}{101.3 \text{ kPa}} \right] \quad (14c)$$

where

$AOTR$ = actual oxygen transfer rate (kg O₂ h⁻¹)

$SOTR$ = standard oxygen transfer rate (kg O₂ h⁻¹)

α = loss correction factor (0.45 unitless)

θ = temperature coefficient (1.024 unitless)

T = temperature of water (°C)

β = oxygen saturation factor (0.95 unitless)

C_{SW} = DO saturation in wastewater (g DO m⁻³)

C_L = aerated liquid DO level (3.0 g DO m⁻³)

C_{ST} = standard p DO saturation in water (9.08 g DO m⁻³)

C_{SS} = standard DO saturation in pure water (g m⁻³)

C_{S20} = standard T DO saturation in water (9.09 g DO m⁻³)

P_b = barometric pressure (101.3 kPa)

DWD = aeration depth (m)

f = effective depth factor (0.3 unitless)

The adopted blower power equation:

$$P_w = \frac{wRT}{8.41e} \left[\left(\frac{p_2}{p_1} \right)^{0.283} - 1 \right] \quad (15)$$

where

P_w = blower power (W)

R = ideal gas constant (8.314 J mol⁻¹ K⁻¹)

T = inlet air temperature (K)

e = blower efficiency (0.65 unitless)

p_2/p_1 = ratio of outlet-to-inlet pressure (unitless)

The analysis specified the implementation of the AIRE-O₂ Triton 3.75 kW model (Figure 10 and Figure 11) for the SBR. The mixer motor provides 2 kW of mixing capacity, whereas the blower provides 1.75 kW for aeration (AIRE-O₂, 2014). The standard powers are suitable with the actual values for a safety factor of 1.2 for both the blower and the mixer.

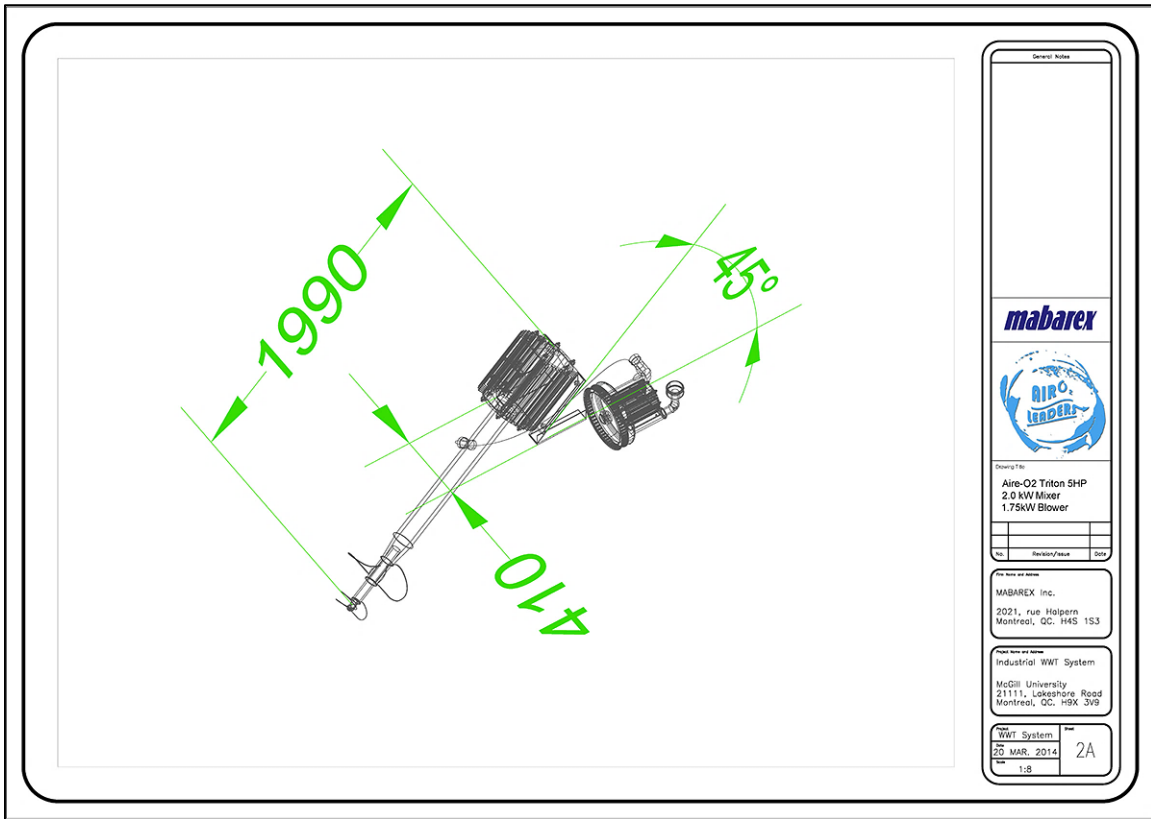


Figure 10. Dimensions and mounting of the Triton™ 3.75 kW model (by Jun Dong)



Figure 11. Illustration of the supplied AIRE-O₂ Triton™ 3.75 kW model (by Jun Dong)

SBR pH Control

During the first anoxic cycle, the denitrification of each mole of nitrate contributes to a mole of hydroxyl ion that shifts the pH to 10.1. The optimal pH for denitrifiers ranges from 7.5 to 9.0 (Glass et al., 1997), but for this project, a pH of 9.0 is specified as it is also optimal for the nutrients recovery by struvite precipitation, which will be recapped in the precipitator specification section on page 18. Furthermore, there is a deficient amount of phosphate necessary to recover most of the ammonium in form of struvite. Thus, phosphoric acid at 73.2 kg $\text{H}_3\text{PO}_4 \text{ d}^{-1}$ was specified to lower the pH while supplying phosphate as a struvite reactant before magnesium is added in the precipitator.

Moreover, during the second aerobic cycle, every mole of ammonium nitrified yields two hydrogen ions that reduce the pH to 1.2. However, the nitrifiers are suitable for a neutral pH (Riera, 2013; Tchobanoglous et al., 2003). Therefore, a pH of 7.0

was specified for the aerobic process with the use of sodium hydroxide. Although lime (CaCO_3) is usually applied as an economical alkalinity source, to ensure high struvite purity, lime was suggested not to be used throughout the treatment system as $\text{Ca}_3(\text{PO}_4)_2$ will be precipitated instead. Consequently, sodium hydroxide was chosen for its acceptable price range, its strong base property and the purity of the struvite that it provides. Chemical simulation specified that 288 kg NaOH d^{-1} should be dosed during nitrification.

Anaerobic Sludge Digester

For small anaerobic sludge digestion applications, a contact high-rate anaerobic sludge digester was specified for a construction design. An overview of the anaerobic sludge digestion processes is presented in Figure 12. The HRT inside an anaerobic sludge digester was specified to be 10 days with 50% sludge digestion at a controlled 35°C mesophilic temperature (Tchobanoglous et al., 2003) for the optimal time, space and economy efficiencies.

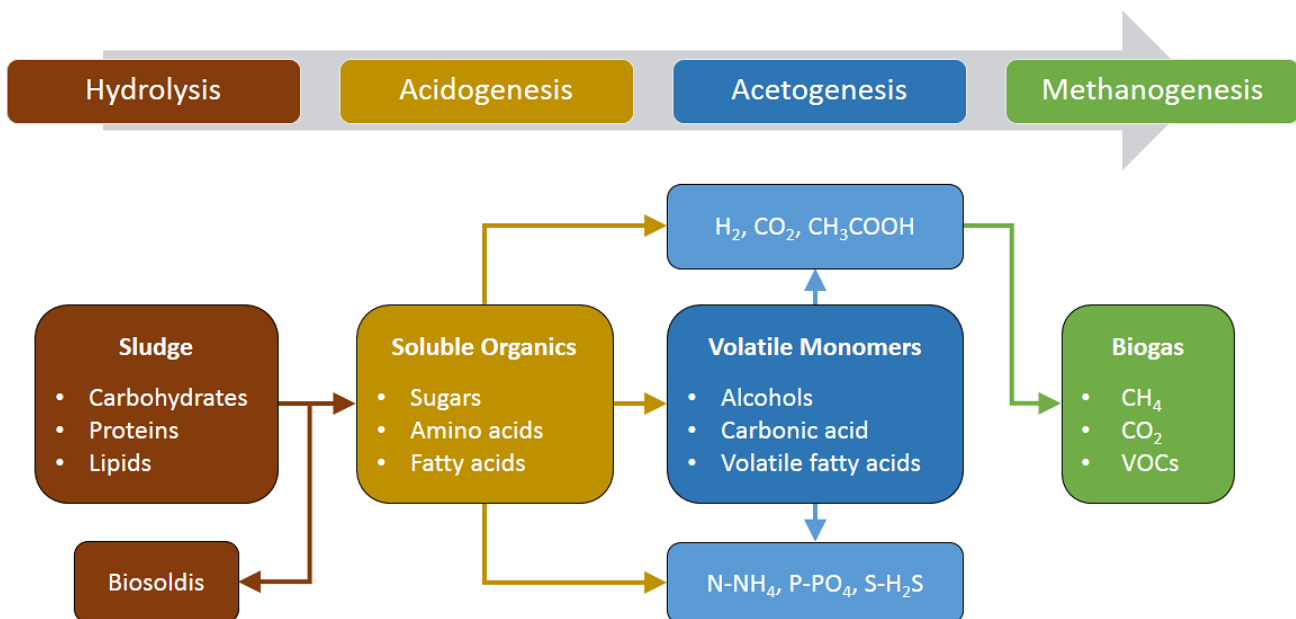


Figure 12. The sludge is subject to different digestion processes shown from left to right. At a controlled temperature of 35°C, the anaerobes take from 10 to 30 days to decompose 50-66% the sludge solids into soluble and volatile monomers. The remaining indigestible biosolids are candidate for fertilizer (by Jun Dong).

Therefore, the anaerobic digester volume was sized similarly with Eq. 1 based on the 10-day HRT and the 10 m³ d⁻¹ sludge flow rate. Furthermore, for a smaller footprint and an adequate mixing efficiency, the digester was specified to be a tall cylinder with a minimum height of 6 meters (Tchobanoglous et al., 2003). As a result, the digester was specified as 100 m³ large with 6 m height and 4.6 diameter (Figure 13 and Figure 14).

For specifying the construction material, the digester heat loss was approximated with Eq. 17 and typical digester material properties and thicknesses. The simulation specified the winter conditions of -25°C air temperature, -5°C ground temperature and 6.7 m s⁻¹ wind speed (Howell et al. 2009).

Heat transfer equation:

$$q_{loss} = UA(\Delta T) \quad (17a)$$

$$U = \frac{1}{\sum \frac{1}{h} + \sum \frac{x}{k}} \quad (17b)$$

where

q_{loss} = heat loss (W)

U = thermal conductance (W m⁻² K⁻¹)

A = surface area (m²)

ΔT = temperature difference (K)

h = convective heat transfer coefficient (W m⁻² K⁻¹)

x = conductive material thickness (m)

k = thermal conductivity (W m⁻¹ K⁻¹)

The construction and insulation materials include concrete, steel and slag wool (Tchobanoglous et al., 2003). Their thicknesses were specified and reported in Figure 13 in millimetres.

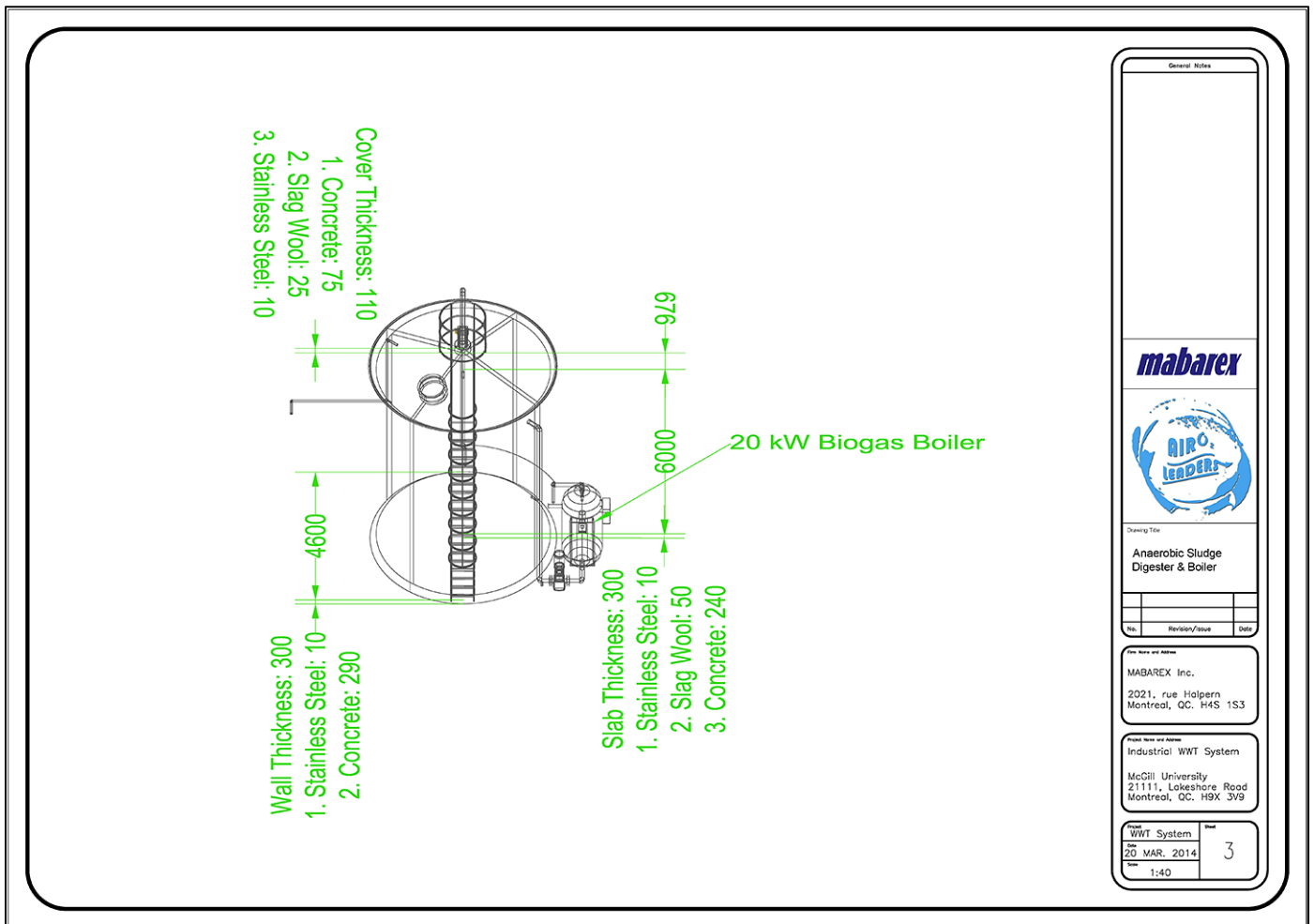


Figure 13. Drawing of the designed anaerobic sludge digester with dimensions for construction (by Jun Dong)



Figure 13. Anaergia provides the manufacture of the designed anaerobic sludge digester (by Jun Dong)

The heat conductivity for the materials and the forced convective heat transfer coefficient (Holman, 2009; Howell et al. 2009) are listed in Table 4 for heat loss simulation. The result of heat loss is ≤ 6.4 kW.

Table 4. Heat transfer parameters

k_{concrete} ($\text{W m}^{-1} \text{K}^{-1}$)	0.8
$k_{\text{stainless steel}}$ ($\text{W m}^{-1} \text{K}^{-1}$)	43
$k_{\text{slag wool}}$ ($\text{W m}^{-1} \text{K}^{-1}$)	0.038
$h_{\text{o, air}}$ ($\text{W m}^{-2} \text{K}^{-1}$)	34

The actual mixing power similarly specified by Eq. 12 is 2.85 kW. The methane produced from the digestion, which was estimated with the following Eq. 16 (Tchobanoglous et al., 2003), has a thermal value of $37.5 \text{ MJ m}^{-3} \text{ CH}_4$ (City of Palo Alto, 2007).

Estimation of methane gas generation:

$$\dot{V} = G_o(Q\Delta S - 1.42P_{X,VSS}) \quad (16a)$$

$$P_{X,VSS} = \frac{QY\Delta S}{1 + k_d(SRT)} \quad (16b)$$

where

\dot{V} = methane generation rate (L d^{-1})

G_o = methane-substrate ratio ($0.4 \text{ L CH}_4 \text{ g}^{-1} \text{ COD}$)

Q = sludge flow rate ($\text{m}^3 \text{ d}^{-1}$)

ΔS = substrate consumption (g COD m^{-3})

P_{VSS} = anaerobes production rate (g VSS d^{-1})

Y = anaerobes yield on COD ($0.08 \text{ g VSS g}^{-1} \text{ COD}$)

k_d = anaerobes death rate (0.03 d^{-1})

SRT = sludge retention time, HRT equivalent (10 d)

From Eq. 16, the consumed amount of substrate (ΔS) was determined by the specific COD released from the sludge dry mass, which is $1.42 \text{ g COD g}^{-1} \text{ VSS}$, multiplied by a typical COD utilisation efficiency of 90% (Tchobanoglous et al., 2003). As a result, 16.8 kW of energy was generated from $38.4 \text{ m}^3 \text{ d}^{-1}$ of methane. For, a 20 kW biogas boiler was specified to the manufacturer as shown in Figure 13. Approximately 7 kW of methane heat was designed to compensate the heat loss for keeping the digester at 35°C , whereas the excess energy was considered to cut other expenses from electrical heating usages in the

slaughterhouse. Moreover, during the digestion, each gram of COD solubilised from the sludge releases 5% of N-NH_4 (Riera, 2013) and 0.5% of P-PO_4 (Bowers, 2007).

Lastly, the digester typically produces carbon dioxide at 30% of partial pressure. Consequently, the carbonic acid is formed by the dissolved carbon dioxide in water (Tchobanoglous et al., 2003). This acidity shall be neutralised by the use of sodium hydroxide. The dosage rate of sodium hydroxide was specified to be $2.6 \text{ kg NaOH d}^{-1}$.

Centrifuge

The centrifuge was specified for a digested sludge flow rate of $10 \text{ m}^3 \text{ d}^{-1}$. The centrifuge model CS10-4 from CENTRISYS (CENTRISYS, 2014), which is displayed in Figure 14 and Figure 15, was selected.

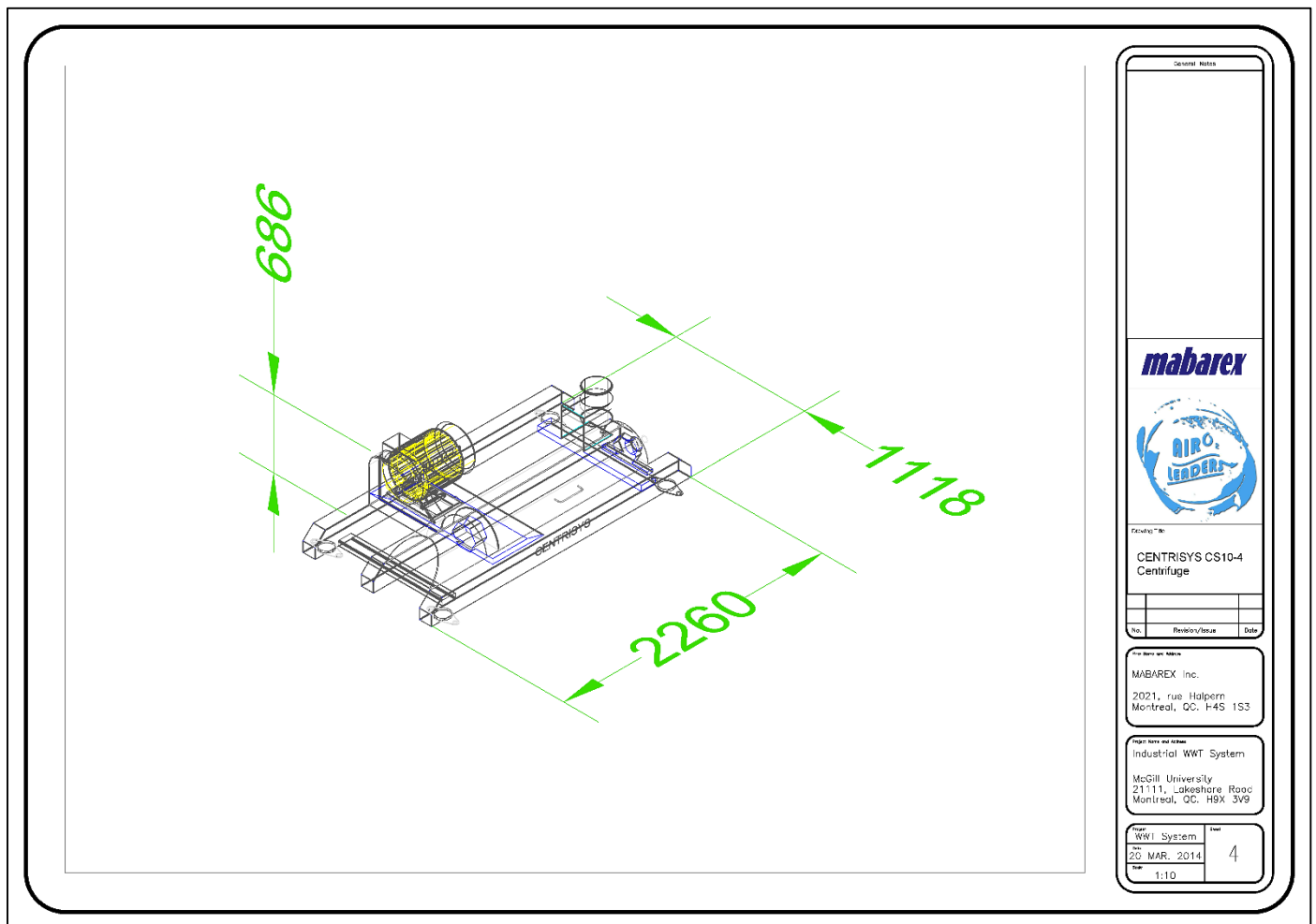


Figure 14. Drawing of the centrifuge with axial dimensions of extremities (by Zhi Li)

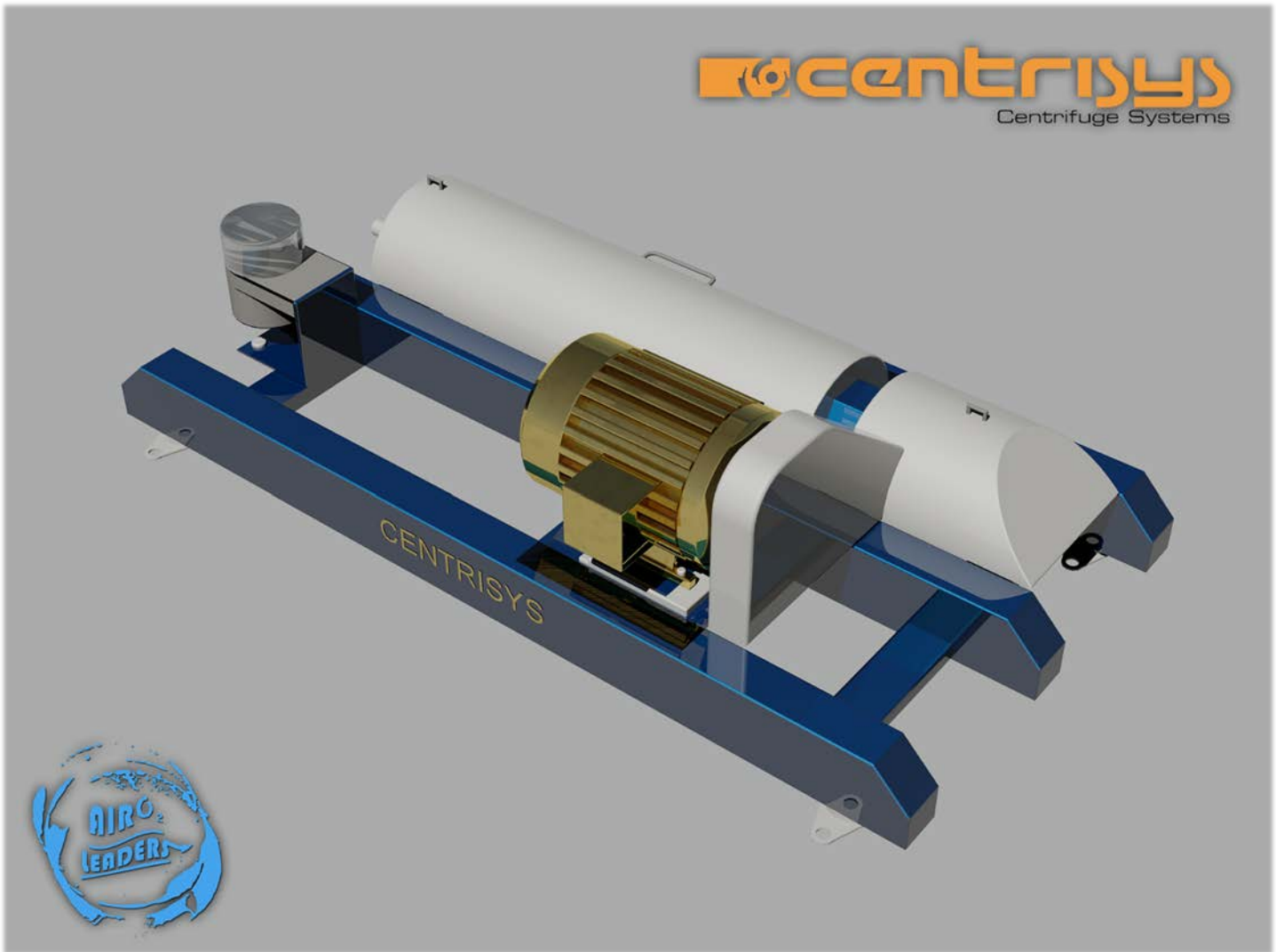
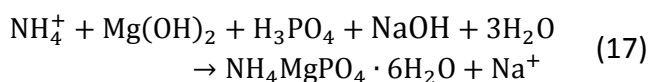


Figure 15. Illustration of the supplied CENTRISYS CS10-4 dewatering centrifuge (by Zhi Li and Jun Dong)

Struvite Precipitator

It is important to recall that the wastewater does not contain enough phosphate to recover most of the ammonium by precipitating struvite. Furthermore, magnesium is also required to start the precipitation. Moreover, a pH of 9.0 is required for the ionisation of phosphate. For the cost efficiency of the reactants, the precipitation reaction, which is represented by Eq. 17, was specified for a pH of 9.



However, the wastewater already contains some dissolved phosphate. As a result, from Eq. 17, less

phosphoric acid will be dosed and the will become greater than 9.0. To mitigate this effect, 20% molar of the magnesium hydroxide was changed to magnesium chloride (MgCl_2) that is weakly acidic. Therefore, the chemical concentration and dose rate was specified as shown in Table 5.

Table 5. Reactant concentrations dose rate

Reactants	Dose rates (kg d ⁻¹)
Mg(OH) ₂	361
MgCl ₂	116
H ₃ PO ₄	487
NaOH	297

Furthermore, the mass-balanced solubility product (Doyle and Parsons, 2002) stated in Eq. 18 solves the amount of struvite precipitated by the desaturation of the reactant concentrations.

$$K_{sp} = ([NH_4^+] - X) ([PO_4^{3-}] - X) ([Mg^{2+}] - X) \quad (18)$$

where

K_{sp} = struvite solubility product ($4.36 \times 10^{-13} \text{ mol}^3 \text{ L}^{-3}$)

$[NH_4^+]$ = ammonium concentration (mol L^{-1})

$[PO_4^{3-}]$ = orthophosphate concentration (mol L^{-1})

$[Mg^{2+}]$ = magnesium concentration (mol L^{-1})

X = struvite formation (mol L^{-1})

The struvite precipitator is selected from Multiform Harvest Inc., a supplier of our client. As found in Figure 16 adopted from Multiform Harvest Inc., the

struvite precipitator was specified as an inverted cone having a 4.55 m height and a 0.91 m wide on top diameter (Bowers, 2009). Thus, each precipitator provides a volume of one cubic meter (1 m^3). A 15-minute HRT was specified (Multiform Harvest Inc., 2013), according to Eq. 1, two precipitators are required to accommodate a $122.3 \text{ m}^3 \text{ d}^{-1}$ precipitation flow while providing a 1.6 safety factor. However, 15-minute HRT was specified only for a conventional struvite precipitation on the post-anerobic stream without the addition of extra phosphate for enhanced ammonium recovery. The future procedure for an optimal specification will be discussed on the Simulation and Optimization section on page 29.

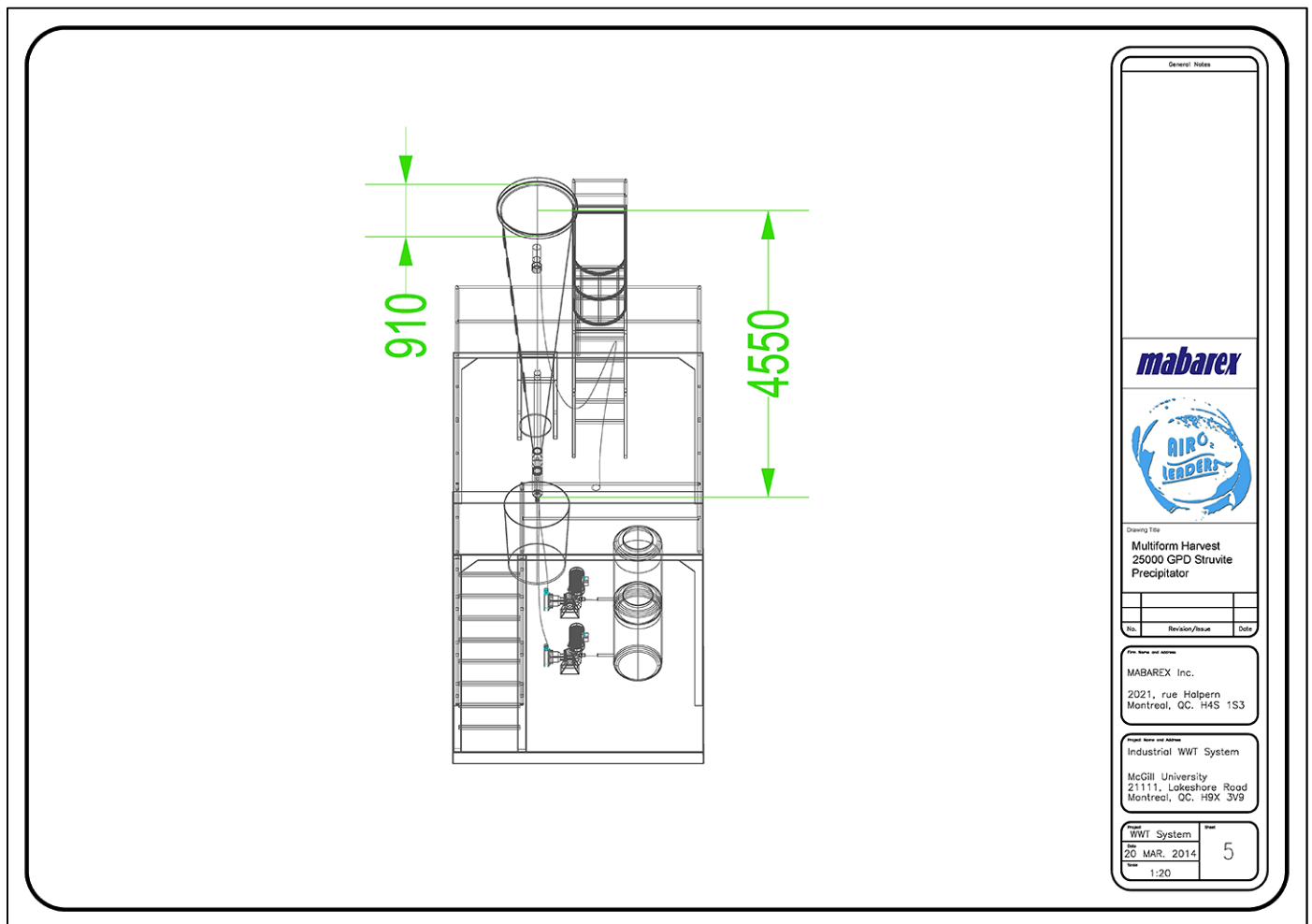


Figure 16. Drawing of the struvite precipitator with its important dimensions (by Jun Dong)

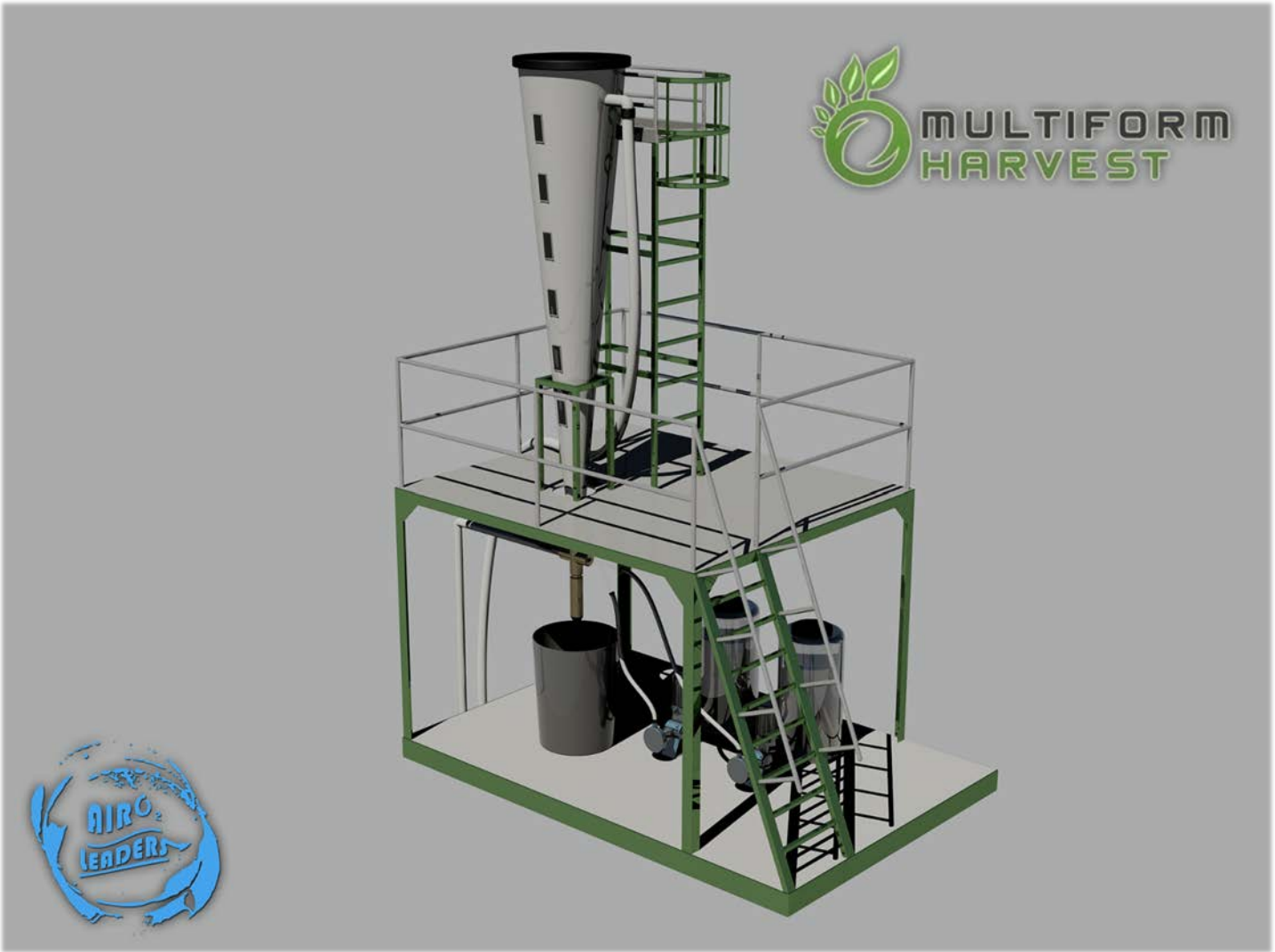


Figure 17. The supplied 25000 GPD struvite precipitator model from Multiform Harvest Inc. (by Jun Dong)

Pumping

The overall pumping power requirement needs to compensate the water elevation difference (static pressure), the flow velocity (dynamic pressure), and the piping friction and bend losses summarized with Eq. 19 and Eq. 20 (Crowe et al., 2009).

The pumping power is computed as:

$$P = \gamma Q h_p \quad (19)$$

where

P = pumping power (W)

γ = fluid specific weight (N m^{-3})

Q = flow rate ($\text{m}^3 \text{s}^{-1}$)

h_p = total pumping pressure head (m)

The head loss within piping is calculated as:

$$h_p = (z_2 - z_1) + \frac{u^2}{2g} \left(1 + \sum K_L + \frac{fL}{D} \right) \quad (20a)$$

$$u = \frac{Q}{\pi \left(\frac{D}{2} \right)^2} \quad (20b)$$

$$f = \frac{64}{Re} = \frac{64}{\left(\frac{4Q}{\pi D \nu} \right)}, \quad (Re \leq 2000) \quad (20c)$$

where

z = water elevation level (m)

u = flow velocity (m s^{-1})

g = acceleration due to gravity (9.81 m s^{-2})

K_L = bend loss coefficient (unitless)

f = friction factor (unitless)
 L = pipe length (m)
 D = pipe diameter (m)
 Re = Reynolds number (unitless)
 ν = kinematic viscosity ($10^{-6} \text{ m}^2 \text{ s}^{-1}$ at 20°C)

After a preliminary analysis, it was important to notice that the flow rate is too low for a significant flow velocity ($u = 0.0013 \text{ m s}^{-1}$) through any pipe. Hence, the power to compensate the dynamic

pressure and the pressure losses become negligible when compared to the static pressure compensation. Moreover, the specific weight for water is 9810 N m^{-3} (Crowe et al., 2009) and 10006 N m^{-3} is for the sludge (Tchobanoglous et al., 2003). Three pumps with their efficiency were chosen by selecting a corresponding flow rate and elevation head from their performance curve (Price Pumps, 2014). These pumps are specified in Table 6.

Table 6. Pumping specifications

Connection	Parameters	Values
Equalization tank to SBR	Pump model	Price RC200 1450RPM 50Hz
	Pump efficiency (%)	38
	Actual power (W)	28
	Standard power (W)	88
SBR to precipitator	Pump model	Price RC200 1750RPM 60Hz
	Pump efficiency (%)	40
	Actual power (W)	58
	Standard power (W)	145
SBR sludge to digester	Pump model	Price LT 2900RPM 50Hz
	Pump efficiency (%)	16
	Actual power (W)	6
	Standard power (W)	36

Simulation and Optimisation

This section is dedicated to explain the procedures that were went through to achieve the preliminary specifications. As physically prototyping of the designed system would require money and more time to build and test, a simulation was performed to generate the preliminary specifications. A simulation software was created on Microsoft Excel VBA by Jun Dong and Zhi Li for a more user-friendly direct analysis, inverse synthesis, optimisation, and instrumentation for the entire wastewater treatment system. However, the modification of calculation algorithms is more difficult compared to its spreadsheet counterpart. Moreover,

computational models are developed on MATLAB Simulink™ by Jun Dong and Dillon Stanger to synthesize all the SBR process timings. These simulations will be explained in the following subsections. In addition, the KTH Visual-MINTEQ 3.1 beta chemical simulation software was used for analysing different chemical equilibria such as for the pH controls and the precipitation of struvite.

The preliminary specifications were generated by the simulations. The simulated results were optimised by carrying out several iterations thereby resulting optimised steady-state specifications. Therefore, the simulation and the optimisation are combined into this one section.

Influent

The influent tab from the VBA software (Figure 18) had provided a direct analysis of the combined influents flow rate and contaminant concentrations. These values then specified, simulated and optimised the system components. The combined influent concentrations were computed by mass balance (Eq. 21).

Mass balance of solute in solvent:

$$C_c Q_c = \sum_{i=1}^3 C_i Q_i \quad (21)$$

where

C_c = combined concentration (g m^{-3})

Q_c = combined flow rate ($\text{m}^3 \text{d}^{-1}$)

i = influent number (unitless)

C_i = concentration of an influent (g m^{-3})

Q_i = flow rate an influent ($\text{m}^3 \text{d}^{-1}$)

Influent Concentrations & Bylaw Limits				Combined Influent
Influent 1	Influent 2	Influent 3	Bylaw Limits	
Q, (m ³ /d) : 85.9	Q, (m ³ /d) : 10.2	Q, (m ³ /d) : 17	Q, (m ³ /d) : N/A	Q, (m ³ /d) : 113.1
COD, (g/m ³) : 7328	COD, (g/m ³) : 23083	COD, (g/m ³) : 1039	COD, (g/m ³) : 800	COD, (g/m ³) : 7804
TKN, (g/m ³) : 2071	TKN, (g/m ³) : 4887	TKN, (g/m ³) : 331.18	TKN, (g/m ³) : 70	TKN, (g/m ³) : 2063
NH ₄ , (g/m ³) : 1630	NH ₄ , (g/m ³) : 2876	NH ₄ , (g/m ³) : 217	NH ₄ , (g/m ³) : 45	NH ₄ , (g/m ³) : 1530
P, (g/m ³) : 0.8	P, (g/m ³) : 728.7	P, (g/m ³) : 0.2	P, (g/m ³) : 20	P, (g/m ³) : 66.4
S, (g/m ³) : 10.9	S, (g/m ³) : 3.1	S, (g/m ³) : 31.8	S, (g/m ³) : 5	S, (g/m ³) : 13.3
FOG, (g/m ³) : 700	FOG, (g/m ³) : 1290	FOG, (g/m ³) : 87	FOG, (g/m ³) : 250	FOG, (g/m ³) : 661
TSS, (g/m ³) : 231	TSS, (g/m ³) : 2580	TSS, (g/m ³) : 57	TSS, (g/m ³) : 500	TSS, (g/m ³) : 417
T, (°C) : 68	T, (°C) : 65	T, (°C) : 65	T, (°C) : 65	TEMP, (°C) : 68
pH : 6.6	pH : 7.3	pH : 7	pH : 6	pH : 6.7
Combined Influent Characteristics sCOD/COD, (%) : 37 bsCOD/COD, (%) : 32 FOG SG, (g/g) : 0.92				sCOD, (g/m ³) : 2887 bsCOD, (g/m ³) : 2497 nsCOD, (g/m ³) : 4917

Figure 18. The blue fields show the input conditions for the original three waste streams. The white fields, which are locked for any unattended modification, are the result of the analysis.

DAF Unit

Referred to Figure 19, the flow rate specified an appropriate DAF unit from the P-TEC MicroDAF series. The specified A-S ratio and the air solubility or s_a (Tchobanoglous et al., 2003) determined the minimum operational air pressure. Moreover, the percent mass contaminant removal was entered.

Although these removal values were adopted from a slaughterhouse DAF case study (Massé and Masse, 2000), a pilot scale chemical analysis on the primary sludge can provide specific values. A 20°C water temperature was assumed after the equalisation tank (Riera, 2014). Lastly, the contaminant removals, the DAF effluent conditions, and the primary sludge flow rate to the digester were computed.

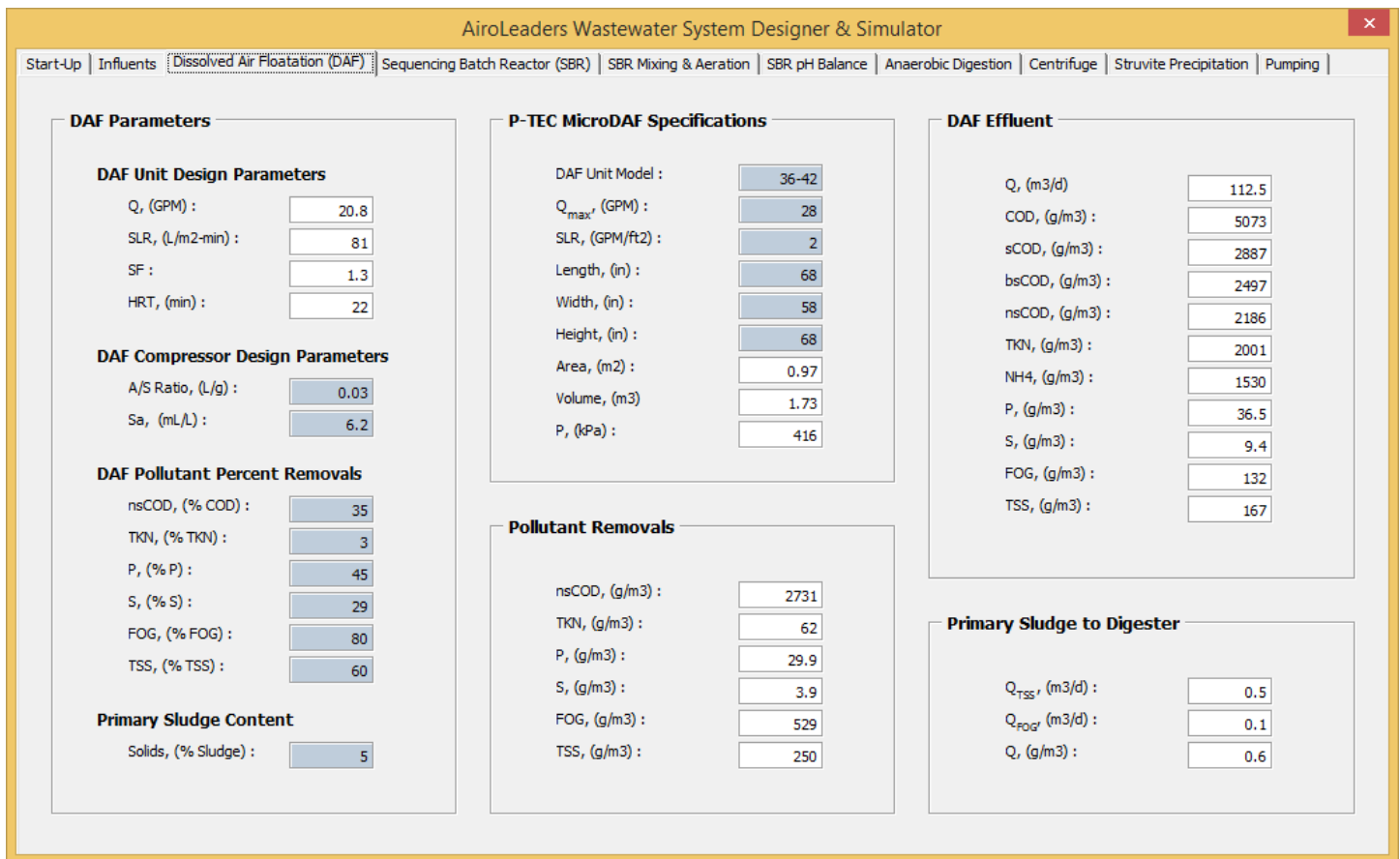


Figure 19. The fields highlighted in blue were filled at once and the white fields automatically displayed important values for analysis and design of the next SBR and the later anaerobic sludge digester.

Dual-Cycle SBR

From the Initial Conditions (Figure 20), the dilution of influent contaminants by the remaining sludge liquid was computed. Furthermore, some of the Design Conditions were specified and the Biokinetics were corrected to the F/M ratio and the temperature. Next, the Anoxic and Aerobic Parameters were input to the computational Monod biokinetics models built on MATLAB Simulink™ as shown from Figure 21 and Figure 22. The simulation then returned the results seen from Figure 23 and Figure 24. These results were entered back to the VBA simulator (the blue fields) for iterating the average sludge production and flow rate, the equilibrium sludge concentration, and the sludge concentration for settling. The sludge concentration was then transferred to the settling model in Figure

25. After the settling simulation, the settling time obtained (Figure 26) was then cited to the VBA simulator for synthesising the process timings and the SBR volumes that are respectively shown in the frames of SBR Process Design and Hextuple SBR Sizing from Figure 20. This process was repeated several times until the optimised steady state values were obtained. The final effluent pollutants were below the limits. The hextuple compartment design of the SBR was suggested by Mabarex Inc. (Riera, 2014) to save construction material. Mabarex Inc. also specified a 100 mm wall thickness (Riera, 2014). Additionally, the central hexagonal island side length of 1.5m was optimised for accommodating the mixer and aerator plus some standing space. The 2m SBR height was optimised for an acceptable settling time, also for the mixer impeller and the aerator diffuser reaching the lowest water level.

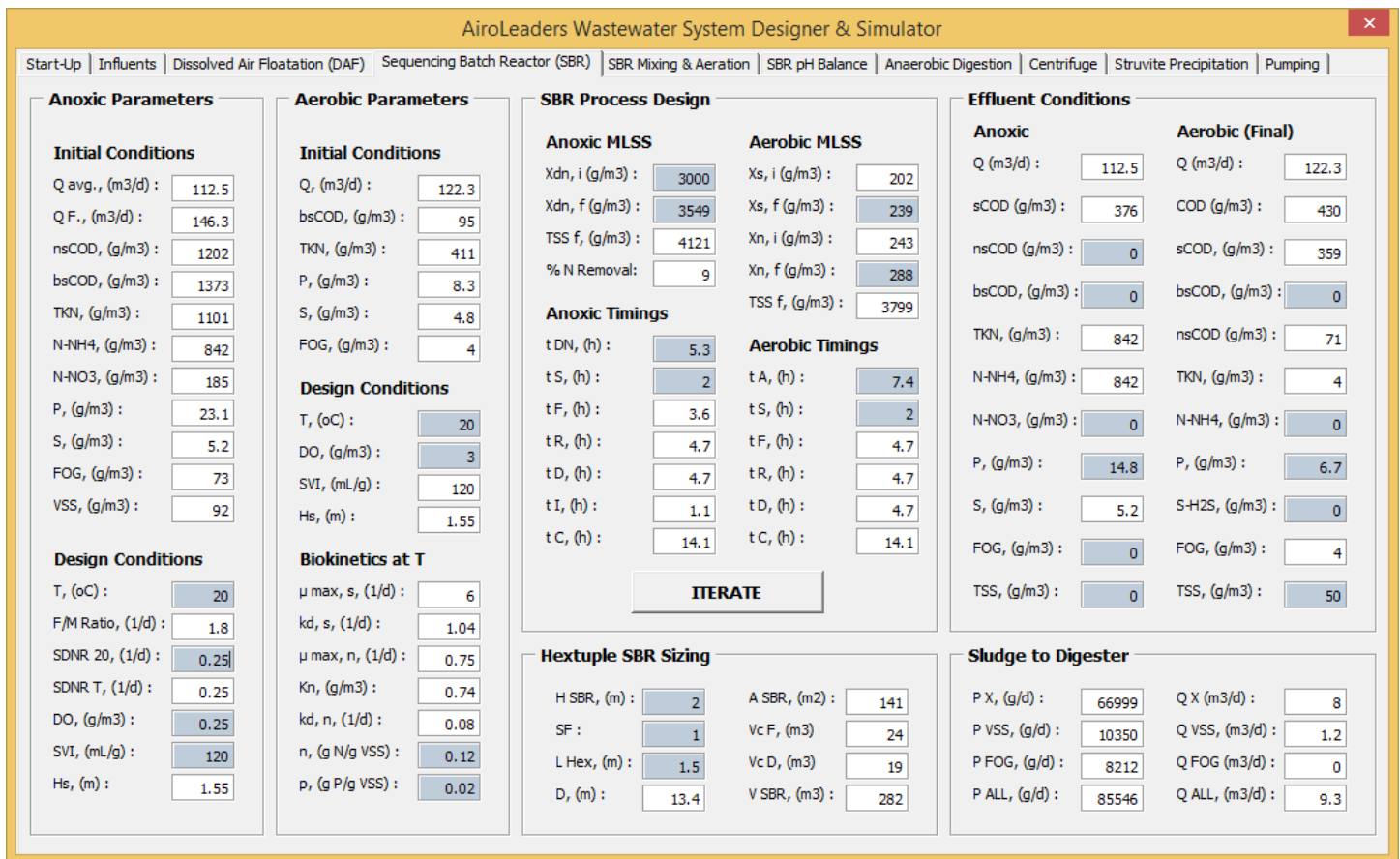


Figure 20. Values from the Parameters and from part of the SBR Process Design frames prepare inputs for the Simulink™ simulation. The remaining blue fields for input are mostly for the Simulink™ simulation results, whereas the remaining white fields show the SBR specifications and the effluent conditions.

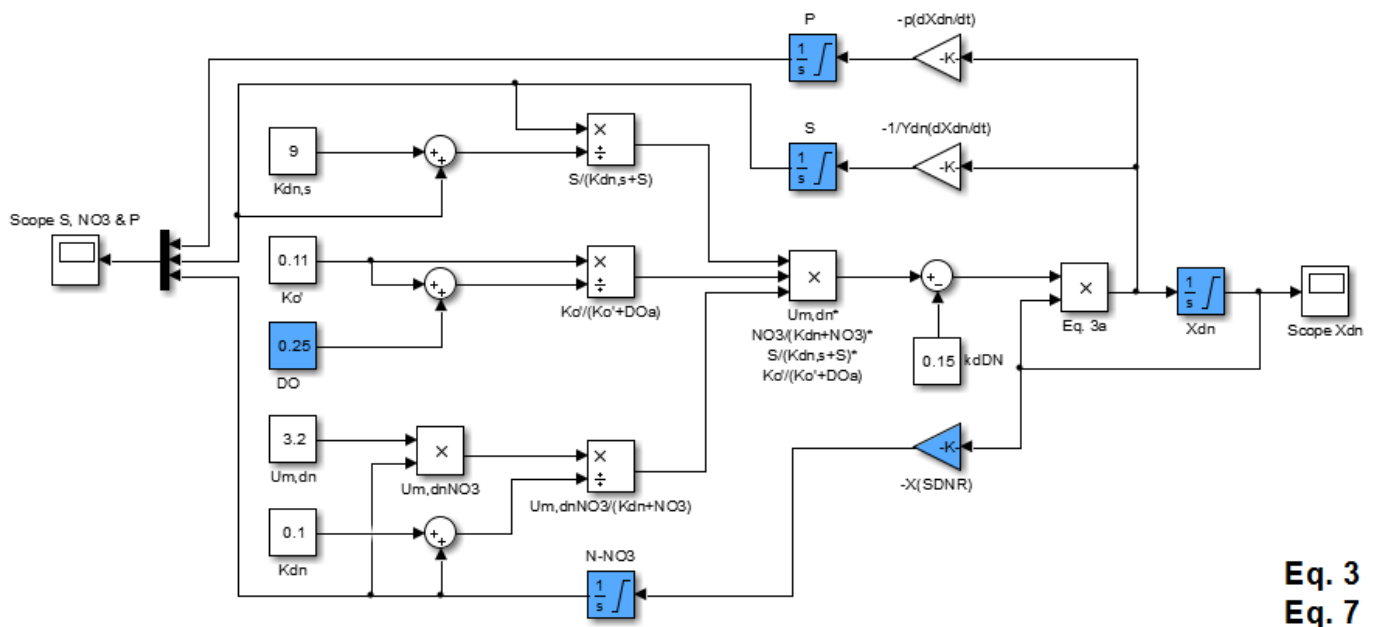


Figure 21. The Simulink™ computational model of Eq. 3 and Eq. 7 simulated the anoxic treatment process. The blue blocks indicate where the values from the VBA simulator should be entered.

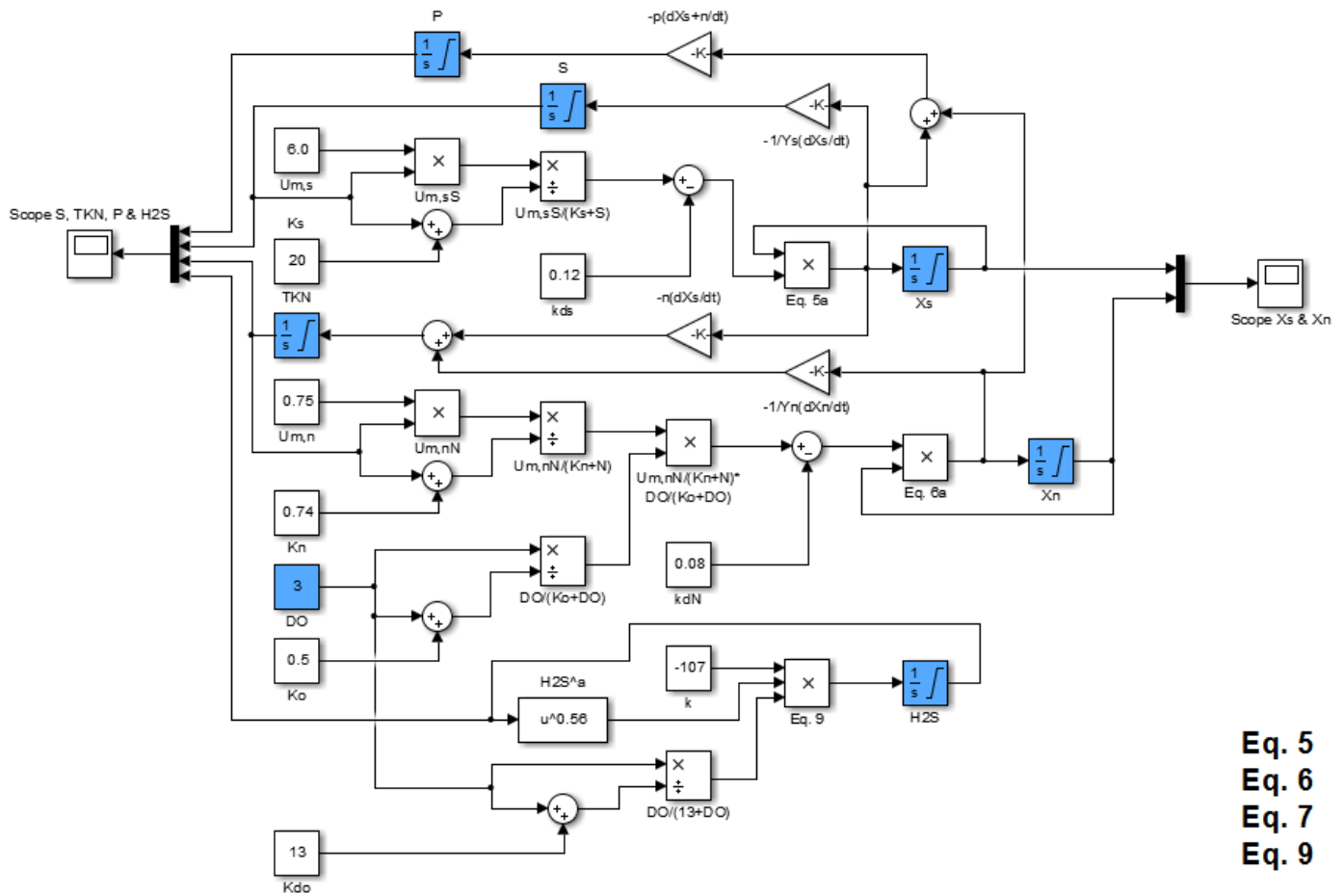


Figure 22. The Simulink™ computational model for simulating the aerobic treatment process; the blue blocks indicate where the values from the VBA simulator should be entered.

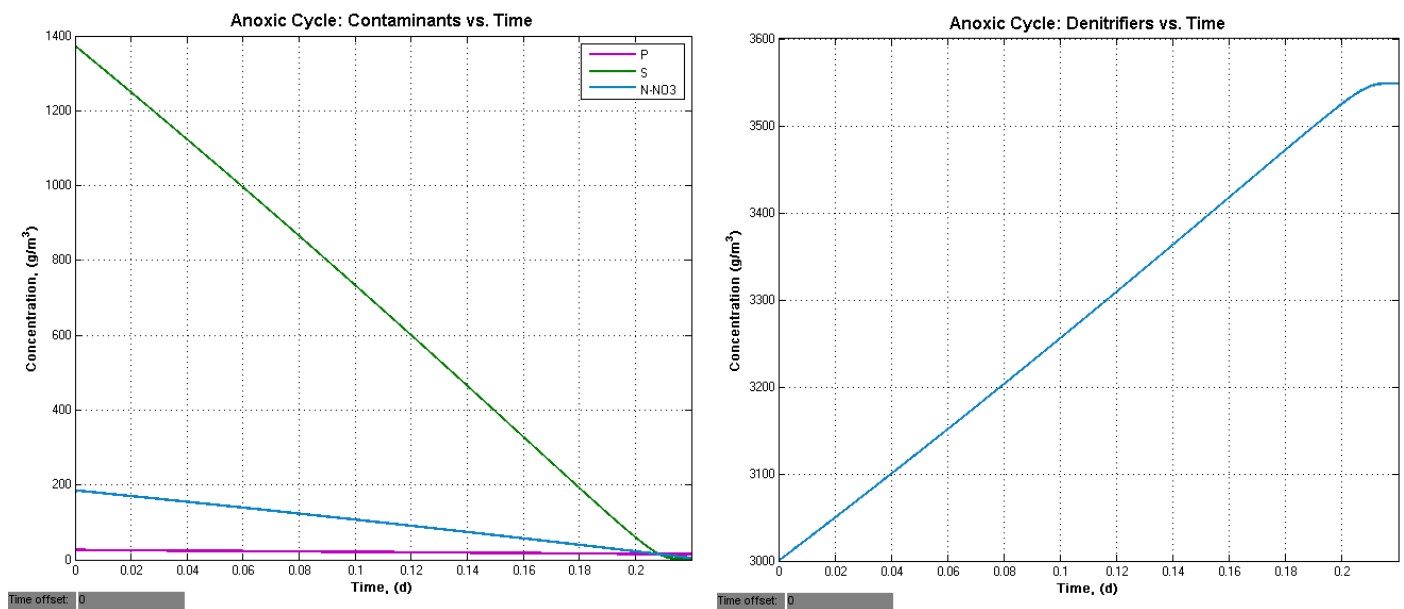


Figure 24. The anoxic timing was obtained from the left graph when the bsCOD (green line) and the N-NO₃ (blue line) converged to 0 g m⁻³. The final denitrifier concentration was obtained from the right side graph.

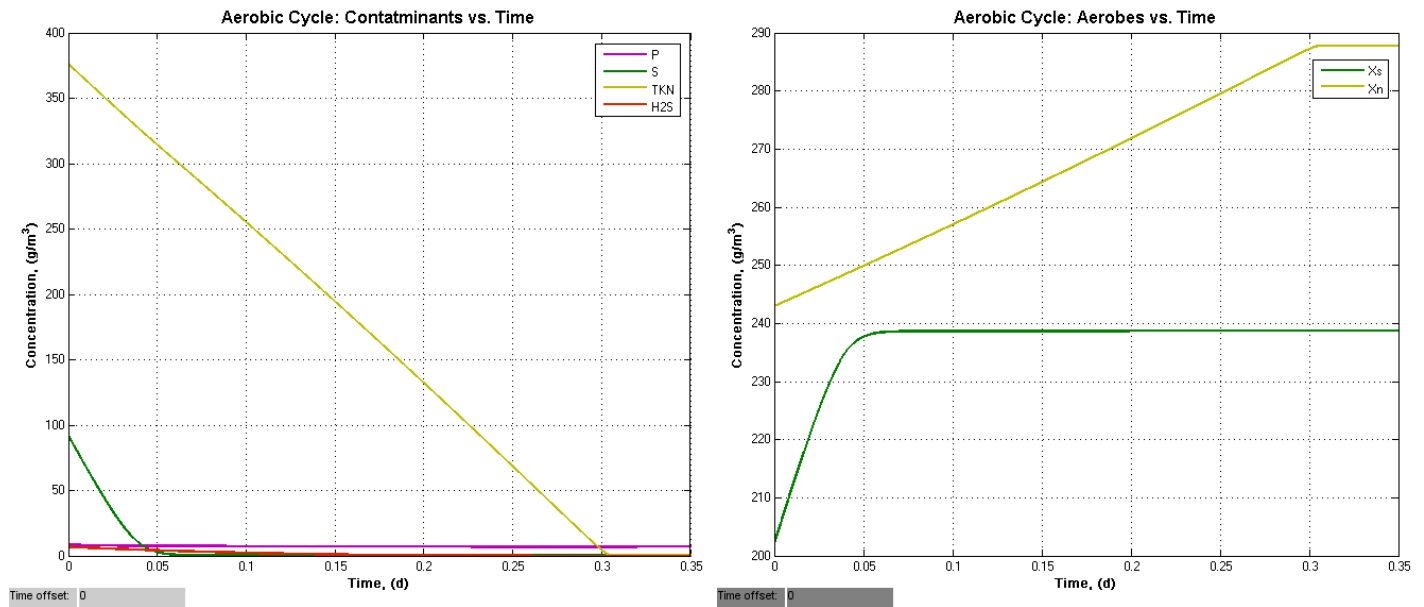


Figure 24. The aerobic timing was obtained from the left graph when the TKN (yellow), bsCOD (green), and the H₂S (red) converged to 0 g m⁻³. The final aerobe concentrations were obtained from the right side graph.

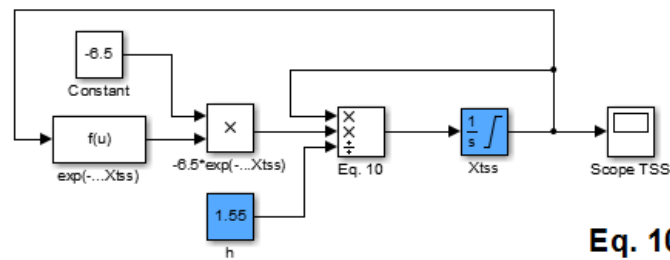


Figure 25. The Simulink™ computational model for simulating the sludge settling; the blue blocks indicate where the values from the VBA simulator should be entered.

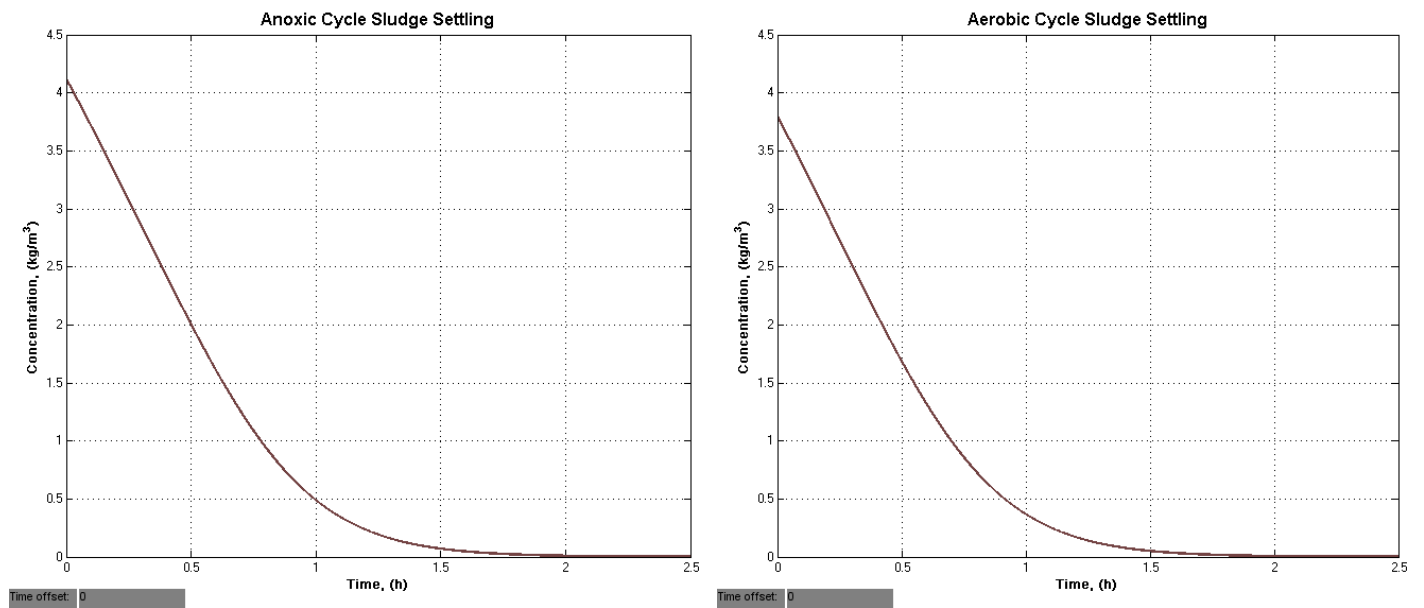


Figure 26. The sludge settling times for the anoxic cycle (left) and the aerobic cycle (right) were obtained when their sludge concentration drops to 0 kg m⁻³.

SBR Mixing and Aeration

The AOTR required for the biological treatments (9 kg O₂ h⁻¹) was automatically optimised by the SBR iteration for steady-state specification. However, due to the wastewater impurities, a minimal 3 g DO m⁻³ required a SOTR of 31 kg O₂ h⁻¹. Hence, the blower should provide 1.43 kW of power. Moreover, a computed minimum power of 1.72 kW should assure an adequate mixing. Additionally, the simulation calculated a total power consumption of 9.74 kW by the SBR as it is always operating with two working mixers and aerators.

SBR pH Control

Referred to Figure 27, the wastewater influent with 6.7 pH was firstly balanced with the SBR sludge,

which having a pH of 7.0, left from the previous aerobic cycle. Thus, the initial anoxic cycle pH became 6.8. Hydroxides were produced during the denitrification, which increased the pH to 10.1. Once the phosphate and the hydrogen ion concentrations are respectively balanced to 6.64E-3 mol PO₄³⁻ L⁻¹ and 0.007 mol H⁺ L⁻¹ with H₃PO₄ supplements, the dosing rate was specified. These concentrations mean that the post-denitrification pH was lowered to 9.0 (Figure 29). Moreover, the aeration of the returned influent produced acids and buffering conjugates (SO₄²⁻). A balanced acid concentration, with the main buffer (SO₄²⁻ and PO₄³⁻) concentrations, simulated for a pH of 7.0 (Figure 30). The concentration difference between the balanced and the produced acids was the sodium hydroxide alkalinity required for specification (Figure 28).

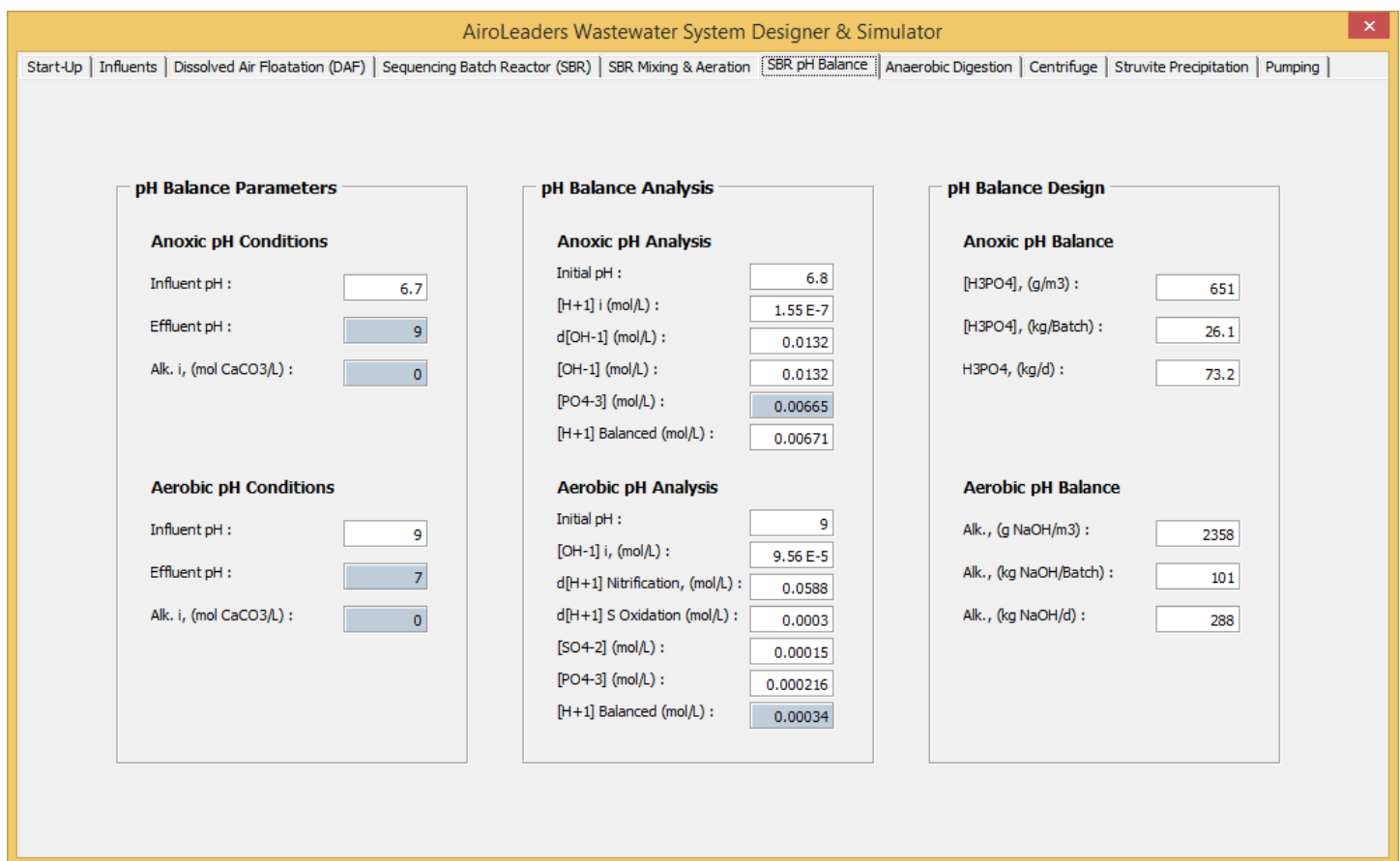


Figure 27. The SBR pH balance was used in conjunction with KTH Visual-MINTEQ for analysing the pH change during the anoxic and the aerobic cycles, so that the pH controls were specified.

No. of iterations

pH

Ionic strength

Sum of cations (eq/kg)

Sum of anions (eq/kg)

Charge difference (%)

Concentrations and activities of aqueous inorganic species (mol / l)

	Concentration	Activity	Log activity
H+1	1.0882E-09	9.6937E-10	-9.014
H2PO4-	7.2537E-05	6.4617E-05	-4.190
H3PO4	8.3388E-12	8.3642E-12	-11.078
HPO4-2	6.5729E-03	4.1390E-03	-2.383
OH-	7.9408E-06	7.0737E-06	-5.150
PO4-3	4.5975E-06	1.6240E-06	-5.789

Figure 29. The simulated results from KTH Visual-MINTEQ showing the balanced anoxic pH along with other buffers at equilibrium

No. of iterations

pH

Ionic strength

Sum of cations (eq/kg)

Sum of anions (eq/kg)

Charge difference (%)

Concentrations and activities of aqueous inorganic species (mol / l)

	Concentration	Activity	Log activity
H+1	9.2997E-08	9.0570E-08	-7.043
H2PO4-	1.2398E-04	1.2074E-04	-3.918
H3PO4	1.4601E-09	1.4603E-09	-8.836
HPO4-2	9.2017E-05	8.2779E-05	-4.082
HSO4-	1.0685E-09	1.0406E-09	-8.983
OH-	7.7756E-08	7.5726E-08	-7.121
PO4-3	4.4106E-10	3.4763E-10	-9.459
SO4-2	1.5000E-04	1.3494E-04	-3.870

Figure 30. The simulated results from KTH Visual-MINTEQ showing the balanced aerobic pH along with other buffers at equilibrium

Anaerobic Sludge Digester

The simulation (Figure 31) computed the total sludge flow from the DAF unit and the SBR into the anaerobic sludge digester. With the specified HRT and digester height, the digester was sized. Furthermore, the percent sludge digestion and the sludge composition analysed the contaminants released into the liquid. This analysis, for optimising the digester and the precipitator, automatically updated every time the SBR specification is iterated. These released contaminants calculated the methane production and the effluent conditions. Moreover, the structural profile was designed and the heat loss from the digester was analysed in the Heat Transfer frame. The heat transfer analysis showed that the designed structural profile has comparative heat conductance and resistance to the

conventional digesters (Tchobanoglous et al., 2003). The heat loss accounts for about 38% heat production from the methane. In addition, the mixing power, which accounts for about 17% of the methane heat production, was computed. As a result, the digester is generating net energy at 7.6 kW. Regarding the pH, the carbon dioxide partial pressure and its Henry constant solved the dissolved carbonic acid content. With the help of Visual-MINTEQ, the amount of sodium hydroxide was specified.

Centrifuge

The centrifuge is running at 15 kW of power while separating 45.2 kg of biosolids per day from the digested sludge liquid. The extracted biosolids has a moisture content of about 60% and that dewatering process discharges 9.8 m³ d⁻¹ of water.

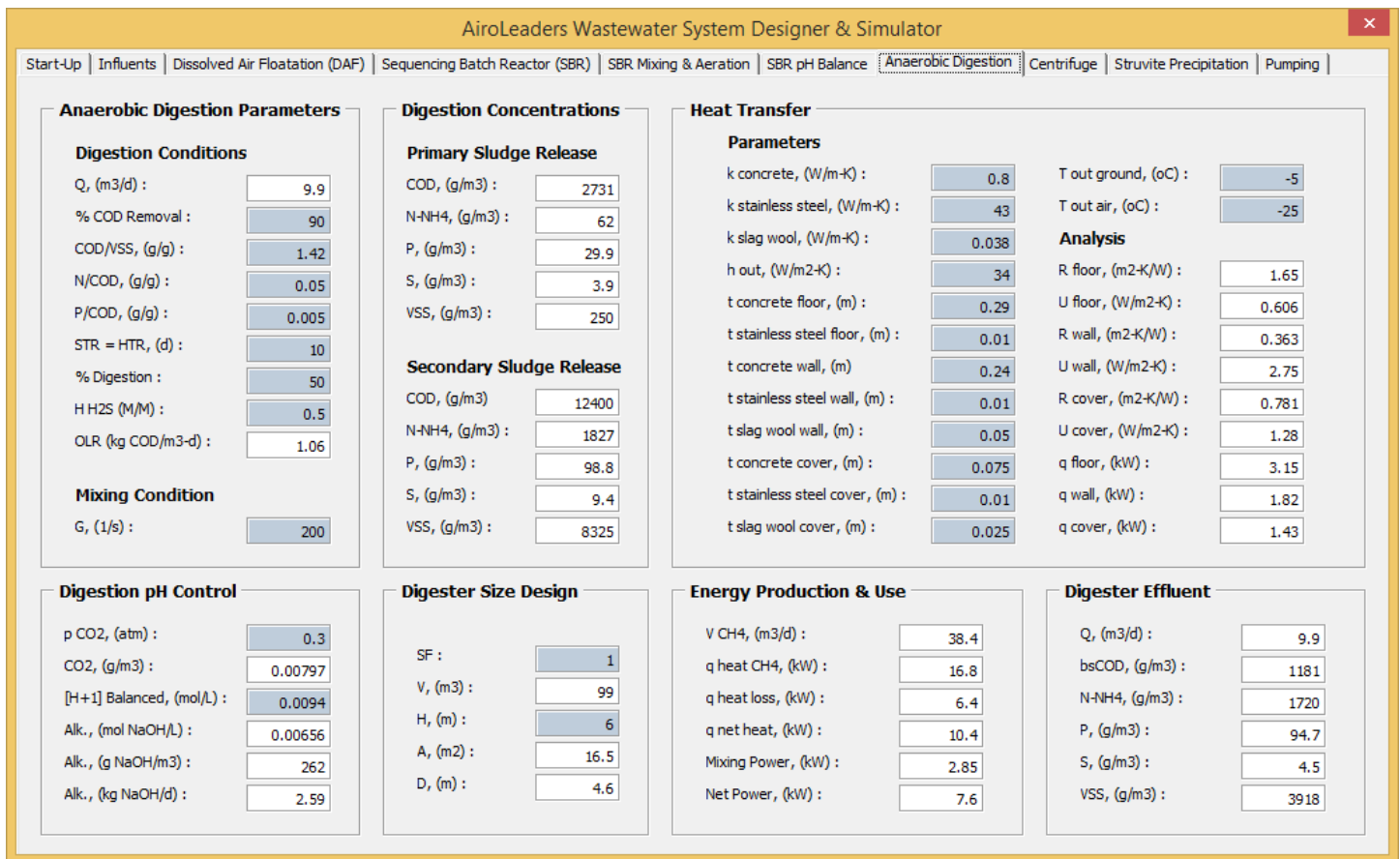


Figure 31. Summary of numerical inputs (blue) and results (white) for analysing and designing the digester

Struvite Precipitator

The combined flow rate, the initial concentration of NH_4^+ and PO_4^{3-} , and the initial pH are firstly computed from the Precipitation Parameters frame (Figure 32). Based on the HRT, the precipitator was specified. For the analysis, the reactive phosphate and magnesium concentrations are specified by a molar ratio equal to one (1). This specification must be optimised after every iteration carried out for the SBR to assure enough NH_4^+ leaves to the SBR to produce enough NO_3^- for the SBR denitrification. Furthermore, based on the reactive concentrations, the desaturation concentration is inversely simulated. The desaturation (molar removal from Figure 32) determined that 1815 kg pf struvite could be produced per day. The revenue from this production is presented in the Safety and Economics

section on page 33. Moreover, the desaturation defined the dose rate for each reactants.

However, with the specified reactant concentration the Visual-MINTEQ, from Table 7, warned that impurities such as magnesium phosphates would be precipitated along with struvite. This also means that ammonium will not be recovered as it was designed.

Table 7. Saturation of the specified precipitation

Mineral	Saturation index
Mg ₃ (PO ₄) ₂ (s)	3.035
MgHPO ₄ :3H ₂ O(s)	0.392
Struvite	2.106

The reason is that the initial reactant concentrations, which are shown in the Precipitation Analysis frame from Figure 32, became too high due to the specified reactant dose rates into the precipitator. To mitigate the impurities, the reactant dose rates shall be

distributed into more precipitators, reducing the reactant concentrations inside a single precipitator. By doing so, the HRT will be prolonged than the one specified by the supplier stated on page 19. This prolonged HRT is acceptable because, as mentioned before on page 19, the supplier did not optimised their HRT based on the conditions of this project.

Consequently, the optimisation of implementing the precipitators and their HRT shall be conducted using the pilot-scaled struvite precipitator also supplied from Multiform Harvest Inc. to our client Mabarex Inc. The precipitation of struvite with external source of phosphate is being studied by engineers and a chemist from our client Mabarex Inc.

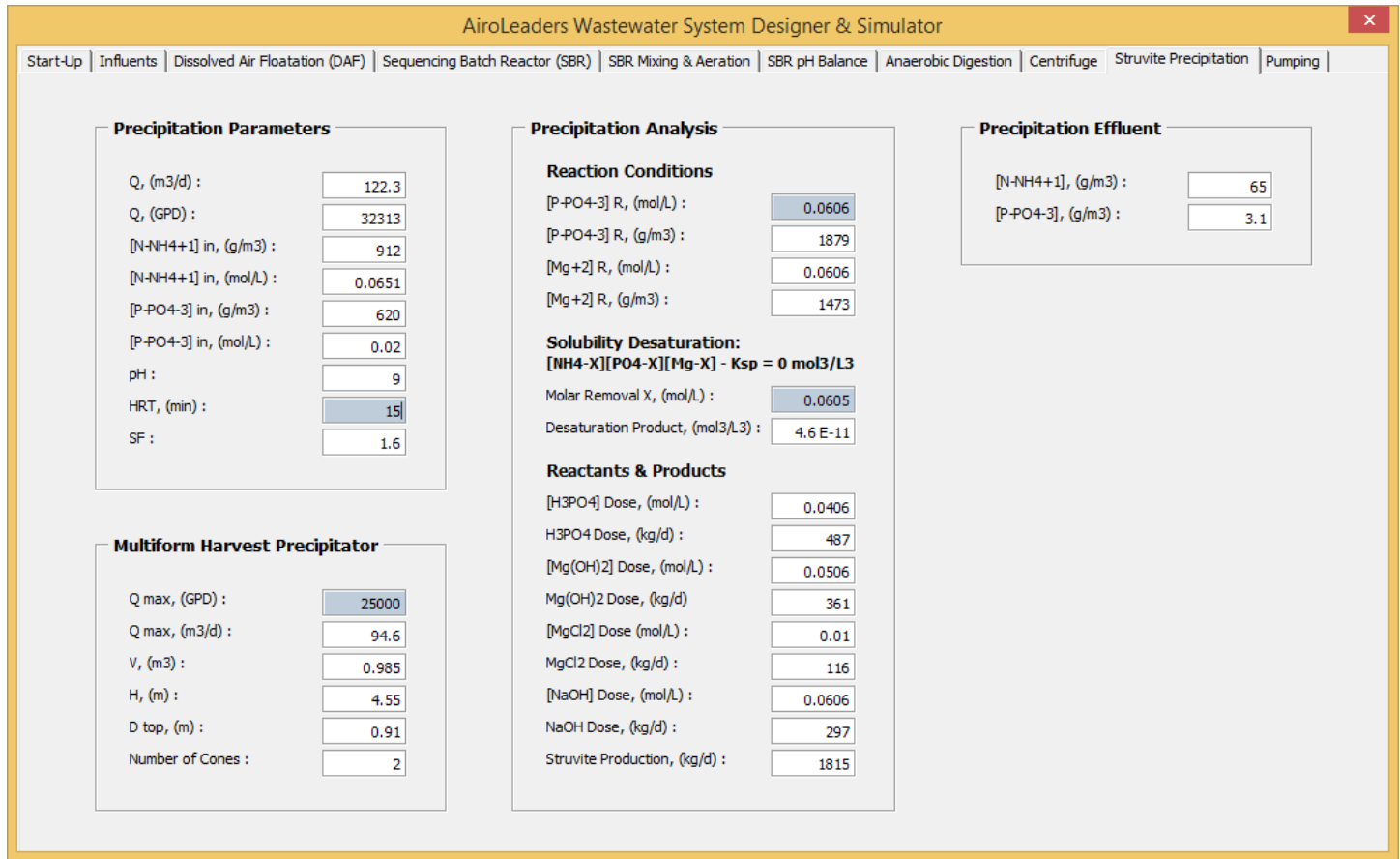


Figure 32. Summary of specifications (in blue) and results (in white) for the struvite precipitation

Testing and Optimisation

The preliminary simulation results were verified by our mentors and compared with typical values from the literature (Tchobanoglous et al., 2003). Three problems were identified which related to the denitrification process, the aeration capacity, and the pH control. These problems, described below, were solved and the corrected parameters were included in the specifications presented.

The first problem was a misinterpretation on the nitrate concentration unit for the denitrification. Instead, the unit should be the mass of nitrogen from the nitrate over volume (g N-NO₃/m³) rather than the mass of nitrate over volume (g NO₃⁻/m³). The readjustment had been made in the simulation. However, the simulation result showed a small 10 g N-NO₃/m³ shortage in completely removing the bsCOD from the anoxic cycle. This problem was fixed by adding less phosphoric acid and magnesium to the precipitator. This modification reduced the

formation of struvite slightly. Thus, more ammonium was left and then nitrified into nitrate during the aerobic cycle for the next denitrification cycle. Nevertheless, the simulated nitrification time did not show a significant increase, so that the optimized process timings and the size of the SBR were kept.

The aeration problem was that the individual blower power of 80W was considered too low and inaccurate by both mentors. The first cause was that the calculation of SOTR ($\text{kg O}_2 \text{ h}^{-1}$) did not consider the fouling and the pressure drop effects on the air diffuser. The second cause was that the SOTR was not converted into airflow rate when calculating the blower power by using the SOTE factor (it is the mass flow of oxygen dissolved into water from the mass flow of air). After readjustments, the preliminary optimised aeration and mixing specifications were simulated as stated previously on pages 12 and 27.

The last problem concerned the pH control. The source of alkalinity was originally specified as lime (CaCO_3). However, as mentioned in SBR pH Control on page 14, lime was replaced by sodium hydroxide (NaOH) to avoid impurities in the struvite.

Safety and Economics

This section will discuss some of the sustainability aspects of the designed wastewater treatment system. These sustainability aspects include effects on the environment, the occupational health and safety, and the economics; the designed system refers to the schematic in Figure 1 on page 4 and the anticipated system setup illustrated on the cover page. Moreover, some of the possible solutions to those sustainability problems will be presented.

Environmental Safety

Typically, any separation of suspended solids, such as the VSS or the sludge, from the wastewater

involves the possible use biological recalcitrant chemical polymers or charged particles to enhance the separation performance (Tchobanoglous et al., 2003). Possible target system components for the application of chemicals include the DAF unit, the SBR and the centrifuge. However, these system components presented above were designed not to utilize chemicals. These components only rely on their physical removal of suspended solids at the costs of lower removal capacity for the DAF unit, longer sludge settling time for the SBR, and a more powerful centrifuge.

Only pH control and struvite precipitation utilize chemicals. The chemicals are derivatives of natural minerals. Furthermore, struvite ($\text{NH}_4\text{MgPO}_4 \cdot 6\text{H}_2\text{O}$) is also a mineral found in nature which the authors have not found to have any known negative environmental impact (Westerman et al., 2009). However, struvite crystals accumulated in animals can eventually block their urinary tract. Thus, the produced struvite should be stored and applied safely so that no animal or child can ingest it. For soil fertilisation, the release of nutrients is gradual from the surface of struvite crystals and the release rate can be controlled through crystal sizing. Smaller struvite particles release more nutrients from the first 3 to 6 weeks than the larger ones (Westerman et al., 2009). Therefore, nutrient runoff can be reduced. However, struvite cannot replace conventional fertilisers as it has a fixed one-to-one molar ratio of N and P, it lacks other nutrients such as potassium, and it may saturate the soil with magnesium (essential for chlorophyll synthesis in plant growth).

One problem is that a biogas scrubber was not specified with the anaerobic digester to remove the volatile part of hydrogen sulfide. The combustion of hydrogen sulfide will produce sulfur oxides that are responsible for acid rains. For further works should

specify a biogas scrubber before the combustion takes place.

Occupational Health and Safety

Railing guards are implemented to most of the locations where falling is possible. Furthermore, the moving parts from the most of the equipment are covered for preventing potential injuries. The only exception is at the center island of the SBR where the mixer, aerator and the catwalk are mounted and where the operator performs maintenance. The problem there is that railing guards cannot be installed to prevent the operator from falling into a SBR compartment and being injured by a mixer in operation. The reason for this problem is that the uninstalation of mixer and aerator in case of replacement should not be hindered and the catwalk should be rotatable all around the SBR. This risk can be eliminated by anchoring the operator to the catwalk. The use of a mask is advised when maintaining the SBR as the dissolved ammonium and hydrogen sulfide are volatile and cause odour.

Moreover, the digester produces anaerobic compost as biosolids fertiliser that may contain opportunistic anaerobic pathogens. To mitigate the biohazard from handling the biosolids, either the system shall include a biosolids pasteurisation system using the excess methane as its heat source, or the operator shall be advised to use gloves, goggles and a mask.

Economics

The capital costs of the designed system (Riera, 2014; Raboud, 2014) on this stage are listed in Table 5. More capital expenses on the precipitators shall be foreseen as more of them will be required.

Table 5. List of components and capital costs

Items	Quantity	Costs (CAD)
DAF Unit	1	50 000
SBR in Concrete	1	160 000
SBR Catwalk	1	30 000
SBR Aerator & Mixer	6	6 X 15 000
Anaerobic Sludge Digester	1	900 000
Centrifuge	1	320 000
Struvite Precipitator	2	2 X 85 000
Total		1 720 000

From table 5, the capital costs are high on the digester and centrifuge. However, they are necessary for attenuating the effect on greenhouse gas emissions while producing more fertilisers as addressed before.

The following Table 6 is a list of specific price in Canadian or US dollars for consumables and goods produced from the operation.

Table 6. List of specific prices

Item	Specific Value	Unit
Electricity ^a	0.0488	¢ kWh ⁻¹
Biosolids ^b	250	\$ ton ⁻¹
Mg(OH) ₂ ^c	150	\$ ton ⁻¹
MgCl ₂ ^d	100	\$ ton ⁻¹
H ₃ PO ₄ ^e	700	\$ ton ⁻¹
NaOH ^f	325	\$ ton ⁻¹
Struvite ^g	1042	\$ ton ⁻¹

The specific prices from Table 6 are multiplied by their corresponding unit production or consumption for determining their yearly revenue or expense from the operation. These values are listed in Table 7.

^a (Hydro-Quebec, 2013)

^b (Parry, 2012)

^c (Wang, 2014)

^d (Yang, 2014)

^e (Wu, 2014)

^f (Liu, 2014)

^g (Seymour, 2009)

Table 7. Summary of the operational revenues, expenses and net profit

Items	Quantity	Revenues (\$/year)	Expenses (\$/year)
DAF Power	9.32 kW		3 984
SBR Operating Power	9.71 kW		4 150
Anoxic pH Control	73.2 kg H ₃ PO ₄ /day		18 704
Aerobic pH Control	289 kg NaOH/day		34 232
Digester Mixing Power	2.85 kW		1 219
Digester pH Control	2.6 kg NaOH/day		307
Digester Net Heat Output	10.4 kW		(4 447)
Centrifuge Power	15 kW		6 412
Biosolids Production	45.2 kg/day	4 126	
Struvite Reactants	487 kg H ₃ PO ₄ /day		124 374
	361 kg Mg(OH) ₂ /day		19 768
	116 kg MgCl ₂ /day		4 249
	297 kg NaOH/day		34 076
Struvite Production	1815 kg struvite/day	690 423	
Pumping Power	0.3 kW		115
Wages: Manager	For 1 person		70 000
Wages: Operators	For 4 people		4 X 40 000
Subtotal		694 549	479 461
Pre-Tax Profit		215 088	

Regarding to Table 7, the wastewater treatment plant will need one (1) professional manager and four (4) operators. One of the operator shall operate the DAF unit and the centrifuge, whereas each from the others shall operate one of the remaining components. The salary for a wastewater treatment plant manager and an operator are respectively about 70 000 \$ per year (Salary.com, 2014) and 40 000 \$ per year (Academicinvest.com, 2011).

In sum, the revenues were mostly from the struvite production, whereas the expenses were mostly from the chemicals and the wages. This wastewater treatment system seemed having a profit potential of 215 000 \$ per year instead of deficit estimated to be -57 000 \$ per year as normal methods (such as the DAF unit plus the SBR) do. The estimated profit

will pay the capital expenses back in a minimum of 8 years or longer if more precipitators will be needed.

Conclusion

To conclude, an innovative wastewater treatment system was designed for the given problem and objectives. This system includes a DAF unit, a dual-cycle SBR, an anaerobic sludge digester, a centrifuge, and at least two struvite precipitators. Their preliminary specifications and analytical results were produced through simulation and optimisations. The designed system, reviewed by the professional mentors, is able reduce the contaminant concentration beyond the bylaw requirements. Furthermore, this environmental friendly system is able to recover nutrients dissolved in the wastewater and to create a net profit.

However, before the implementation of this innovative design, time-consuming physical pilot-scale studies should be expensed and conducted to validate the accuracy of the preliminary specifications and the simulated analytical results. For instance, the DAF unit performance must be assessed with the actual wastewater from the particular slaughterhouse. The effluent from the DAF unit pilot-scale study will feed in batches a pilot-scale single compartment SBR (instead of a hextuple-compartment SBR for a continuous feeding) to verify the dual-cycle SBR performance and effluent conditions for less expense. The sludge from the DAF unit and the pilot-scale SBR will then be continuously sent into a downscaled anaerobic sludge digester to determine an accurate HRT, percent digestion, methane production, and the effluent conditions. Finally, a single pilot-scale struvite precipitator will determine an appropriate HRT, precipitator number, and reactant concentrations or dose rates to minimise the impurity in the struvite product. Once the final specifications and results from the physical prototyping are determined, the component manufacturing can then be started.

Design Paper Competition

Currently, our team is participated in a design paper competition sponsored by the Water Environment Federation (WEF), an international organisation that represents experts in the water engineering industry, and by the Réseau Environnement from the province of Quebec in Canada. The team member, Dillon Stanger, was elected by the team to register for that competition. The competition registration was

accepted on the week starting on the 9th of February 2014. The design competition paper can be prepared and submitted in 3 months starting from the submission date of this design report stated on the cover page.

Acknowledgements

We would like to deeply and sincerely to express our gratitude to Mr. Ignacio Riera, Mr. Carlos Sanchez Barrios, and Mr. Jean-Philippe Raboud for spending their precious time and resources helping our team through this design project. Their mentorship had brought us valuable knowledge for creating ideas facing new challenges in the sustainability of wastewater treatment. This honourable experience shall be remembered. We also like to thank our professor Dr. Grant Clark for his guidance on the design process through his instructions, his constructive comments and his direct answers to questions.

Mabarex Inc.

- Ignacio Riera, Eng., M. Eng. Applications Engineer, iriera@mabarex.com
- Carlos Sanchez Barrios, Eng., M. Sc., Project Manager, csanchez@mabarex.com
- Jean-Philippe Raboud, Eng., Ph.D., Engineering Director, jpraboud@mabarex.com

McGill University

- Olivier Grant Clark, Ph. D., P. Eng., Associate Professor, grant.clark@mcgill.ca

References

- AcademicInves.com. 2011. How to Become a Wastewater Operator. Available at: <http://www.academicinvest.com/science-careers/environmental-science-careers/how-to-become-a-wastewater-operator>. Accessed 21 March 2014.
- AIRE-O₂. 2004. AIRE-O₂ Triton Process Aerator/Mixer. MN: AIRE-O₂ Aeration Industries
- Bowers, K. E. [Multiform Harvest Inc.]. 2007. Fluidized Bed Crystallizer for Phosphorus Removal and Production of Granular Struvite Fertilizer. *Harvesting Clean Energy Conference and Biodiesel in the Northwest workshop*. Idaho: DoubleTree Riverside Hotel
- Bowers, K. E. [Multiform Harvest Inc.]. 2009. A NEW CONCEPT FOR REMOVAL OF PHOSPHORUS FROM DAIRY FARM WASTE. Washington D.C.: USDA Research, Education & Economics Information System
- CENTRISYS. 2014. Centrisys Dewatering Centrifuges. WI: CENTRISYS Co.
- City of Palo Alto. 2007. Numbers, Numbers, Numbers. Available at: <http://archive.cityofpaloalto.org>. Accessed: 28 February 2014
- Clark, O. G. 2014. Personal conversation. Montreal, QC: Macdonald Campus of McGill University.
- Communauté métropolitaine de Montréal [CMM]. 2008. Règlement numéro 2008-47 sur l'assainissement des eaux. Quebec: Montreal
- De Nardi, I. R. 2008. Performance evaluation and operating strategies of dissolved-air flotation system treating poultry slaughterhouse wastewater. *Resources, Conservation and Recycling*, Vol.52 – Issue 3
- Doyle, J. D., and S. A. Parsons. 2002. Struvite formation, control and recovery. *Water Research* 36(16):3925-3940
- Feedlot Services Australia [FSA]. 2002. Case Study 11 – Dissolved Air Floatation. Queensland: FSA Environmental
- Glass, C., J. Silverstein. 1997. Denitrification kinetics of high nitrate concentration water: pH effect on inhibition and nitrite accumulation. *Water Research*, Vol. 32 – Issue 3
- Hydro-Quebec. 2013. Comparison of Electricity Prices in Major North American Cities. QC: Hydro-Quebec.
- Liu, I. 2014. Competitive price wholesale Caustic Soda Flakes NaOH. Available at: http://www.alibaba.com/product-detail/Competitive-price-wholesale-Caustic-Soda-Flakes_1354924843.html. Accessed 18 March 2014
- Massé, D. I., L. Masse. 2000. Characterization of wastewater from hog slaughterhouses in Eastern Canada and evaluation of their in-plant wastewater treatment systems. *Canadian Agricultural Engineering*, Vol. 42, No. 3.
- Ministère du Développement durable, de l'Environnement, de la Faune et des Parcs [MDDEFP]. 2001. Guide pour l'étude des technologies conventionnelles de traitement des eaux usées d'origine domestique. Quebec, QC : Gouvernement du Québec
- Multiform Harvest Inc. 2013. Designed to Meet Your Needs with a Hassle-Free and Flexible Implementation Approach. Seattle, WA: Multiform Harvest Inc.
- Parry, D. 2012. A Look at the Economics of Biosolids. MA: CDM Smith.
- Piedmont Technical Services [P-TEC]. 2014. MicroDAF Capacities from 12 GPM to 80 GPM. Piedmont, QC: Piedmont Technical Services
- Price Pumps. 2014. Select a Close-Coupled Centrifugal Pump. Available at: http://www.pricepump.com/cen_pumps.aspx. Accessed: 20 March 2014.
- Riera, I. 2014. Personal communication. Montreal, QC: Mabarex Inc.
- Raboud, J.-P. 2014. Personal communication. Montreal, QC: Mabarex Inc.
- Salary.com. 2014. Waste Water Treatment Plant Manager - U.S. National Averages. Available at: <http://www1.salary.com/Waste-Water-Treatment-Plant-Manager-Salary.html>. Accessed 21 March 2014.
- Sharma, K. R., and Z.Yuan. 2010. Kinetics of chemical sulfide oxidation under high dissolved oxygen levels. In *SPN6, Sixth International Conference on Sewer Processes and Networks*. Surfers Paradise, Gold Coast, Australia.
- Seymour, D. 2009. Can Nutrient Recovery Be a Financially Sustainable Development Objective? Washington D. C.: Kennedy/Jenks Consultants.
- Stenstrom, M. K., D. Rosso. 2010. Aeration. LA: University of California
- Tchobanoglous, G., F. L. Burton, Stensel, H.D [Metcalf & Eddy, Inc.]. 2003. Wastewater Engineering – Treatment and Reuse, 4th Edition. NY: McGraw-Hill

- Wang, J. 2014. Magnesium Hydroxide. Available at:
http://www.alibaba.com/product-gs/202005267/Magnesium_Hydroxide.html. Accessed 23 February 2014.
- Westerman, P. W., K. D. Zering, Rashash, D. 2009. Struvite Crystallizer for Recovering Phosphorus from Lagoon and Digester Liquid. *North Carolina State University and A&T University Cooperative Extension*, 10/09—VB/KEL.
- Wu, M. 2014. Phosphoric Acid. Available at:
http://www.alibaba.com/product-gs/297192894/Phosphoric_Acid.html. Accessed 23 February 2014
- Yang, A. 2014. Magnesium Chloride, Good Quality, Factory Price. Available at: http://www.alibaba.com/product-gs/753491128/2013_HOT_Magnesium_Chloride_good_quality.html. Accessed 23 February 2014